

CERENKOV COUNTER TECHNIQUE IN HIGH-ENERGY PHYSICS

J. Litt and R. Meunier¹

CERN, Geneva, Switzerland

CONTENTS

1	INTRODUCTION.....	1
2	GENERAL PROBLEMS ASSOCIATED WITH THE DETECTION OF CERENKOV RADIATION..	3
2.1	<i>The Small Light Yield</i>	3
2.2	<i>Quantum Efficiency and Noise</i>	3
2.3	<i>Choice of Cerenkov Angle and Radiator</i>	5
2.4	<i>Attainment of Prescribed Refractive Index</i>	8
2.5	<i>Optical Dispersion in the Radiator</i>	8
2.6	<i>Optical Aberrations</i>	9
2.7	<i>Energy Loss, Scattering, and Diffraction Effects</i>	11
2.8	<i>Phase Space Acceptance</i>	12
3	THRESHOLD CERENKOV COUNTER.....	14
4	DIFFERENTIAL CERENKOV COUNTER.....	19
4.1	<i>Differential Counter using a Solid or Liquid Radiator</i>	19
4.2	<i>Differential Gas Counter</i>	23
4.3	<i>Optically Corrected Gas Differential Counter</i>	25
5	COMPARISON OF THRESHOLD AND DIFFERENTIAL CERENKOV COUNTERS.....	29
6	PATTERN RECOGNITION IN A FOCUSING CERENKOV COUNTER.....	34
6.1	<i>Ring Image Detector</i>	34
6.2	<i>Spot Image Detector</i>	37
6.3	<i>Multiplexed Cerenkov Counter</i>	39
7	CONCLUSIONS.....	40

1 INTRODUCTION

Following the discovery of Cerenkov radiation in 1934 by Vavilov (1) and Cerenkov (1) and the subsequent theoretical explanation by Tamm & Frank (2) in 1937, a great deal of effort has been put into the investigation of the properties of this phenomenon and its application. Several review articles have appeared (3) that cover the whole subject of Cerenkov radiation in great detail. The aim of the present article is to supplement the previous reviews by placing emphasis on the recent developments in the Cerenkov counter technique as applied to the physics research at high-energy accelerators. The applications to cosmic ray research and to the measurement of total deposited energy, such as in shower detectors, will not be reviewed (3).

¹ Visitor from CEN, Saclay, France.

Tamm & Frank (2) developed a classical theory to account for Cerenkov radiation based on the idea that a charged particle moving in a transparent medium with a uniform velocity larger than the velocity of light in the medium emits a radiation along a conical wavefront. The angle of emission θ of the radiation of a given wavelength λ is related to the relative velocity $\beta (=v/c)$ of the particle and the refractive index n of the medium by the relation

$$\cos \theta(\lambda) = 1/\beta n(\lambda) \quad 1.$$

The theory also produced the spectral distribution and hence the intensity of the radiation. These predictions were confirmed experimentally by Cerenkov (4), and there followed a quantum-mechanical theory of the effect by Ginsburg (5) in 1940.

Relation 1 can be rewritten as

$$\cos \theta(\lambda) = v_{\text{light}}(\lambda)/v_{\text{particle}} \quad 2.$$

which shows that the angle of emission of the light is directly related to the ratio of the velocity of the light in the radiator to the particle velocity. This fact explains the usefulness of Cerenkov radiation in the field of elementary particle physics. The optical measurement of the emission angle of the light together with the knowledge or measurement of the velocity of light in the same medium affords the means of determining the velocity of a particle and its direction within the accuracy of optical techniques.

For a high-energy charged particle, the measurement of its relative velocity β together with a measurement of its momentum p is practically the only way to determine the mass m of the particle, which is deduced from the relation

$$\begin{aligned} m = p/\beta\gamma & \quad \text{with} \quad \gamma = (1 - \beta^2)^{-\frac{1}{2}} \\ \text{and} \quad c = 1 & \end{aligned} \quad 3.$$

By using the Cerenkov effect, the velocity β can be measured to an accuracy in the range of 10^{-2} to 10^{-7} , with an accuracy in m for a single particle given by

$$dm/m = \gamma^2(d\beta/\beta) + (dp/p) \quad 4.$$

A Cerenkov counter consists of a transparent medium (gaseous, liquid, or solid) in which the radiation is emitted, and an associated electronic detector. The research at high-energy particle accelerators uses several types of Cerenkov counters which differ in their mechanical arrangements and quality of the optical systems. From relation 1 it is seen that the radiation is not produced unless $\beta n(\lambda) > 1$ (i.e. the Cerenkov angle must be greater than zero). The possibility of detecting particles with velocities above a given value is exploited in the *threshold Cerenkov counter*. An instrument which detects the radiation over a small range of angle at a nominal value θ is known as a *differential Cerenkov counter*.

The Cerenkov effect is the result of an electromagnetic interaction that produces light which can be detected by photomultipliers. Cerenkov detectors, which are standard equipment in high-energy physics experiments, provide a nondestructive method for measuring the mass of individual charged particles.

2 GENERAL PROBLEMS ASSOCIATED WITH THE DETECTION OF CERENKOV RADIATION

2.1 *The Small Light Yield*

The number of Cerenkov photons N_γ emitted per unit length of a radiator of length L in the Tamm-Frank theory is given by

$$dN_\gamma/dL = 2\pi\alpha Z^2 \int_{\lambda_2}^{\lambda_1} [1 - (1/\beta^2 n^2)] (d\lambda/\lambda^2) \quad 5.$$

where α is the fine structure constant ($\sim 1/137$), Ze is the charge of the particle, and λ_1 , λ_2 define the limits of the spectral range of the detected radiation. Relation 5 shows that most of the Cerenkov light appears at small values of λ .

Due to the Z^2 dependence in equation 5, a particle with large charge can produce sufficient Cerenkov light intensity to be recorded on photographic emulsion (6). However for singly charged particles the light yield is quite small: for example, the energy loss by Cerenkov radiation in the wavelength bandwidth from 200 to 600 nm is about 1 keV, which is about 100 times less than the energy loss by ionization. It is therefore most important in a Cerenkov detector to minimize the effect of ionization which can cause some radiators to scintillate, and to detect the Cerenkov radiation over as wide a bandwidth as possible.

Thus, many efforts have been made to improve the light transmission and extend the sensitivity of the photodetector into the ultraviolet region where the light yield is greater. At long wavelengths the detection by the counter is limited simultaneously by the low-energy threshold of the photocathodes and the reduced Cerenkov photon emission as given in equation 5. There is not much to be gained in this region of the spectrum.

In relation 1 the refractive index $n(\lambda)$ and Cerenkov angle $\theta(\lambda)$ are functions of the wavelength λ . Extending the wavelength bandwidth leads to a dispersion $d\theta/d\lambda$ of the Cerenkov light that is detrimental to the precision of the measurement of θ , and hence β . The dispersion can be made smaller by *reducing* the bandwidth using optical filters. However, this is possible only when the flux of particles can compensate for the reduced light yield in a given radiator thickness. For single-particle detection one can either reduce the dispersion by using a smaller value of θ or apply achromatic correction to the optics.

2.2 *Quantum Efficiency and Noise*

Only the best quality photomultipliers or image intensifiers can be considered for use in single-particle detectors. The detection efficiency of a given counter is obtained by folding the quantum efficiency of the photodetector with the optical transmission and the Cerenkov light spectrum.

As a rule, only the specifications of the photocathode efficiency are available from the manufacturers. However, the efficiency for collecting the photoelectrons at the anode depends upon the wavelength of the light, especially at the level for detecting single photoelectrons (7). High-speed photomultipliers collect the photoelectrons by

focusing them onto a small-size first dynode, which is elaborately calculated to minimize transit time differences. Photoelectrons that are emitted with initial energies exceeding a level of about 0.8 eV are likely to miss the first dynode. This occurs for wavelengths shorter than about 450 nm, which is the region of interest for Cerenkov light detection. This effect depends strongly on the magnitude of the accelerating field in the region between the photocathode and the first dynode, although raising the collecting field also increases the noise level of the detector.

This reduction of collection efficiency does not continue at wavelengths shorter than 300 nm because a larger fraction of the photoelectrons is emitted with very low velocities (see Duteil et al, 8); however in this region the detection of Cerenkov light is restricted by the transmission through the material of the counter optics and the entrance window of the photodetector. By using ultraviolet-transmitting materials such as fused silica, the detection of the Cerenkov light can be accomplished out to wavelengths of about 200 nm.

The effective detection efficiency of a photodetector as used in a Cerenkov counter with the associated electronic equipment can be measured if one defines a wavelength bandwidth that would be transmitted by a standard set of optics. It is convenient to define the standard optics as those that would be used in the simplest threshold Cerenkov counter, consisting of (a) one front-aluminized mirror, especially coated for reflection at ultraviolet wavelengths and containing a protective-interference layer of $\lambda/2$ thickness of MgF_2 at 350 nm, and (b) one exit window of ultraviolet-transmitting fused silica which is antireflection coated with a layer of $\lambda/4$ thickness of MgF_2 at 350 nm. These details are not so restrictive, but do introduce the necessary transmission attenuation that would be present in any threshold or differential Cerenkov counter. With this standard optics it is possible to experimentally measure (8) and compare the performances of different types of photomultipliers.

For a Cerenkov counter of length L and Cerenkov angle θ , the number of photoelectrons N produced by the passage of a singly charged high-energy particle is given by

$$N = AL\theta^2 \quad 6.$$

where A characterizes the photodetector taking into account the Cerenkov light spectrum and the transmission of the standard optics. Values of the parameter A have been measured in several laboratories (8) and are in good agreement. The best photomultipliers available today, having a fused silica entrance window and a bi-alkali (K-Cs-Sb) photocathode, have a value of the parameter A from about 100–150 cm^{-1} . Photomultipliers having a photocathode of lower quantum efficiency and a glass entrance window provide a value of A from about 50–60 cm^{-1} .

In a focusing type of Cerenkov counter the light flash associated with a single particle is isochronous for a particle traveling along the counter axis because the time taken by the light is equal to the time of flight of the particle. For particles at a distance from the axis, because the wavefront of the Cerenkov light is conical, the duration of the flash of light is typically a few picoseconds. Hence it is the transit time-spread in the photomultiplier which is the main contributor to the

coincidence resolving time of the Cerenkov detector; this time can be of the order of a few nanoseconds.

The noise pulses in a photomultiplier, mainly arising from single photoelectrons, are indistinguishable from true signals since the threshold for the detection electronics is generally set below this level. Therefore for the differential type of Cerenkov counter the light output is in most cases shared between several photomultipliers, and the output signals are placed in a coincidence arrangement. In this manner the accidental count rate can be reduced to an extremely low level at the expense of reducing the overall counting efficiency of the detector.

2.3 Choice of Cerenkov Angle and Radiator

Since the Cerenkov light is emitted at a given angle θ , it appears to an observer to come from a circle positioned at infinity. Focusing optics can be used to concentrate this light onto a ring image of radius r in the focal plane of the system. The radius r is given by $r = f \tan \theta$, where f is the focal length of the optics. The basic principle of the differential Cerenkov counter is to detect these ring images using diaphragms placed in front of photodetectors. The counter detects the radiation

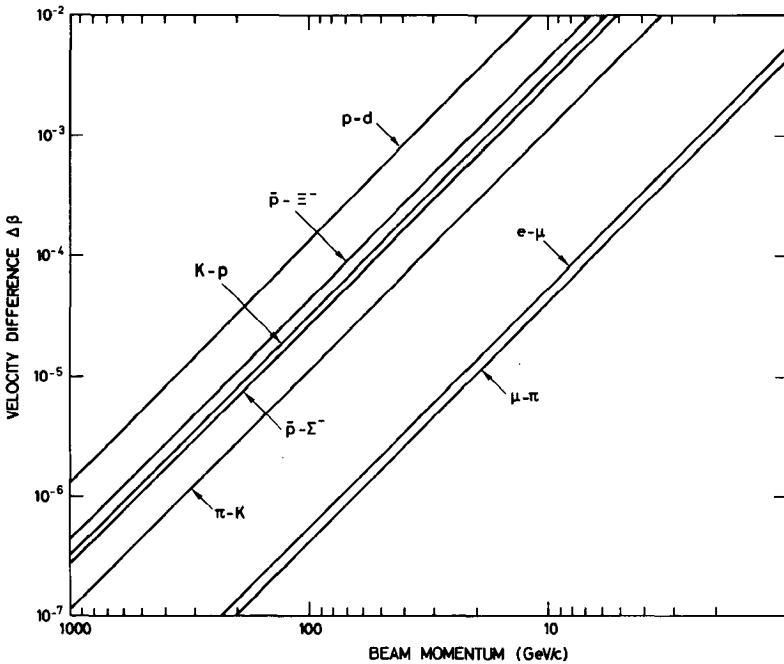


Figure 1 Velocity difference between pairs of particles as a function of the beam momentum.

emitted at a given angle θ and within an angular range of $\Delta\theta$. The velocity resolution $\Delta\beta/\beta$ achieved by such a detector is obtained by differentiating equation 1, and is given by

$$\Delta\beta/\beta = \tan \theta(\lambda)\Delta\theta \quad 7.$$

In a beam of particles of momentum p , the velocity difference between two particles of mass m_0 and m_1 is given by

$$(\Delta\beta/\beta)_{m_0m_1} = (m_1^2 - m_0^2)/2p^2 \quad 8.$$

The velocity differences between different pairs of particles as a function of the beam momentum are indicated in Figure 1. The velocity resolution of a differential counter at the highest beam momentum is normally designed to be *two or three times smaller* than the velocity difference between the particles m_0 and m_1 .

From equation 7 the velocity resolution of a differential counter is proportional to θ and, providing that the optics is well designed, can be improved by reducing $\Delta\theta$. The light output from the counter, from equation 6, is proportional to θ^2 . Thus, the final choice of angle will be a compromise between a required velocity resolution and angular acceptance for a given application, and a minimum tolerable amount of light output for a given size and cost of the device.

In order to achieve a given value of the Cerenkov angle, a suitable material must be chosen for the radiator. Figure 2 shows the variation of the Cerenkov angle for different values of the refractive index n as a function of the particle velocity β , calculated from equation 1. Transparent materials are available for use in Cerenkov counters over the range of n from 1.0 to about 1.8. The different regions of n are obtained by using various materials:

1. $1.0 \lesssim n \lesssim 1.13$ is provided by gases below their critical points (9), and by a

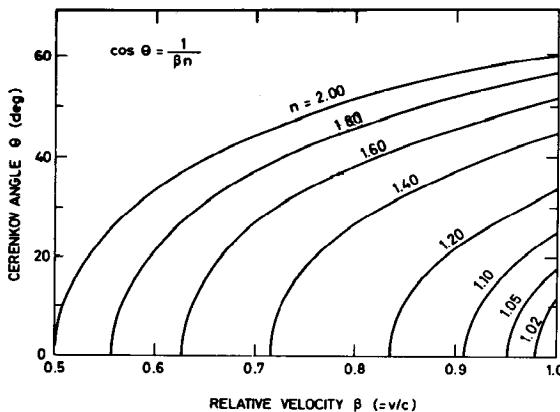


Figure 2 . Variation of the angle θ of emission of Cerenkov radiation for different values of the refractive index n as a function of particle velocity β .

few liquified gases such as $n = 1.11$ for liquid hydrogen and $n = 1.13$ for liquid deuterium.

2. $1.13 \lesssim n \lesssim 1.35$ is provided by gases above their critical points.

3. $1.28 \lesssim n \lesssim 1.33$ is provided by fluorocarbons of quite high density that have high transparency in the ultraviolet and yet low dispersion.

4. $n \gtrsim 1.33$ is provided by many liquids including light hydrocarbons and also water and glycerine mixtures.

5. $n \gtrsim 1.46$ is achieved by many solids such as fused silica, plastics, and glasses.

An inhomogeneous medium can be used in a Cerenkov counter, provided that the scale of the inhomogeneity is small compared to the wavelength of the Cerenkov radiation. The use of a mixture of very fine silica powder and air has been suggested (10) which, by varying the compaction factor, can produce average values of the refractive index in the range from 1.05–1.20.

There are four cases of the application of Cerenkov light to particle velocity determination that can be distinguished:

1. Threshold Cerenkov counter using a solid or liquid radiator: The threshold velocity $\beta_0 = 1/n$ (corresponding to $\theta = 0$) can be quite low. For example, using Plexiglas with $n = 1.50$ produces a threshold value $\beta_0 \gtrsim 0.67$ or $\gamma_0 \gtrsim 1.3$.

2. Threshold gas Cerenkov counter: To obtain high values of n it is often necessary to use extremely high pressures. Hence a reasonable upper limit to the available range of n could be to use ethylene gas at 50 atm, which produces a value $n = 1.13$. This corresponds to a threshold velocity $\beta_0 \gtrsim 0.88$ or $\gamma_0 \gtrsim 2.15$.

3. Differential Cerenkov counter using a solid or liquid radiator: Since this type of counter uses a relatively large value of θ , the velocity resolution cannot be made extremely small by reducing $\Delta\theta$ since the angular acceptance becomes too small for the counter to be useful. The lowest index liquid which is commonly used is FC75 which, for $\Delta\beta/\beta \lesssim 5 \times 10^{-4}$ and $\Delta\theta \sim 10^{-3}$ rad, corresponds to a value $n = 1.28$. Thus the upper limit of β becomes equivalent to particle separation of typically the doublet π, K in beams of up to about 5 GeV/c. The lower limit to β corresponds to the largest n value, which is about 1.58 for styrene or the liquid DC704. Hence this type of counter is approximately restricted to values of $\beta \gtrsim 0.63$ or $\gamma \gtrsim 1.3$.

4. Differential gas Cerenkov counter: These counters have an application in beams up to a few hundred GeV/c, but the lower limit is set by the requirement of using a gas at a reasonable pressure, which results in a limit of approximately $\beta \gtrsim 0.8$ or $\gamma \gtrsim 1.60$.

A gas radiator provides a simple means of changing the refractive index merely by altering the operating pressure. The change of index is given by the Lorentz-Lorenz law:

$$(n^2 - 1)/(n^2 + 2) = (R/M)\rho \quad 9.$$

where R is the molecular refractivity, M is the molecular weight, and ρ is the gas density. For pressures that are not too high, equation 9 can be approximated to high accuracy by

$$(n-1) = (n_0-1)P \quad 10.$$

where n_0 is the refractive index of the gas for a given wavelength of light, at the temperature of the counter, and at a pressure of 1 atm. The pressure P is in atmospheres.

2.4 Attainment of Prescribed Refractive Index

Sufficient precision is required in the value of the refractive index of the radiator to achieve a given velocity resolution $\Delta\beta/\beta$. For low-velocity particles there is no problem with the liquid or solid radiator whose refractive index can be measured to a few parts in 10^4 or 10^5 . The only necessary precaution is taking care of any temperature effects. As the particle velocity increases, so does the required precision of the index measurement. At high energies gases are used as the radiator and knowledge of the refractive index becomes more difficult. The index depends upon the gas density, as given in equation 10, which in turn depends upon the temperature and pressure according to the equation of state. The refractive index can be calculated from a measurement of the gas pressure and temperature, but such a procedure can be seriously affected by any impurity in the gas. Other methods have been used for measuring the refractive index, such as having an oscillating circuit containing a capacitor which is immersed in the gas, although such methods require a refractometer for absolute calibration.

For accurate work the refractive index should be continuously monitored using an interferometer, which directly measures the quantity $(n-1)$ by counting the number of fringes. In this way temperature, pressure, and purity controls are not necessary. This method also leads to an *absolute* determination of the value of β provided that the Cerenkov angle θ is known, as occurs in an achromatic counter.

If one aims at, say, 10 increments of the refractive index setting between the pion and kaon peaks in a mass spectrum for a beam of momentum p , the required accuracy $\Delta n/n$ is given by

$$\Delta n/n \approx \frac{1}{10}(\beta_\pi - \beta_K)/\beta_\pi \approx (m_K^2 - m_\pi^2)/20p^2 \quad 11.$$

where m_π, m_K are the masses of the pion and kaon, respectively. Hence for

$$\begin{aligned} p = 200 \text{ GeV}/c & \quad \Delta n/n = 2.8 \times 10^{-7} \\ p = 300 \text{ GeV}/c & \quad \Delta n/n = 1.2 \times 10^{-7} \\ p = 400 \text{ GeV}/c & \quad \Delta n/n = 7.0 \times 10^{-8} \end{aligned}$$

With a Rayleigh type of refractometer, an accuracy $\Delta n/n$ of better than 10^{-7} can be achieved.

2.5 Optical Dispersion in the Radiator

In equation 1 the Cerenkov angle θ is given as a function of the wavelength λ of the light. Hence there is a spread (dispersion) of the Cerenkov angle due to the variation of the refractive index of the radiator as a function of λ . The amount of chromatic dispersion $\Delta\theta_{\text{DISP}}$ is given by differentiating equation 1.

$$\Delta\theta_{\text{DISP}} = \Delta n / [n(\lambda) \tan \theta(\lambda)] \quad 12.$$

where Δn is the change in refractive index over the range of wavelengths. If one defines an average wavelength λ_2 (which is the mean of the distribution of detected photoelectrons versus wavelength), and wavelengths λ_1, λ_3 , which are the means of the distributions on either side of the average wavelength, then equation 12 can be rewritten as:

$$\Delta\theta_{\text{DISP}} = [n(\lambda_2) - 1] / [n(\lambda_2)v \tan \theta(\lambda_2)] \quad 13.$$

where

$$v = [n(\lambda_2) - 1] / [n(\lambda_1) - n(\lambda_3)] \quad 14.$$

The parameter v characterizes the optical dispersion in the radiator and is a quantity having the same definition as the Abbe number for glasses but for the wavelength of interest in Cerenkov detectors. Table 1 contains values of the parameter v and refractive index for some commonly used gas radiators. The wavelengths chosen are those that are compatible with fused silica optics and S13 or S133 photocathode spectral response. These values merely illustrate the variation of these parameters for typical gases. An exhaustive list of the physical quantities of radiator materials can be found in the review articles by Jelley (3) and Zrelov (3).

2.6 Optical Aberrations

Typical optical systems for a threshold and differential Cerenkov counter are illustrated in Figure 3. In the threshold counter, the Cerenkov light is focused by

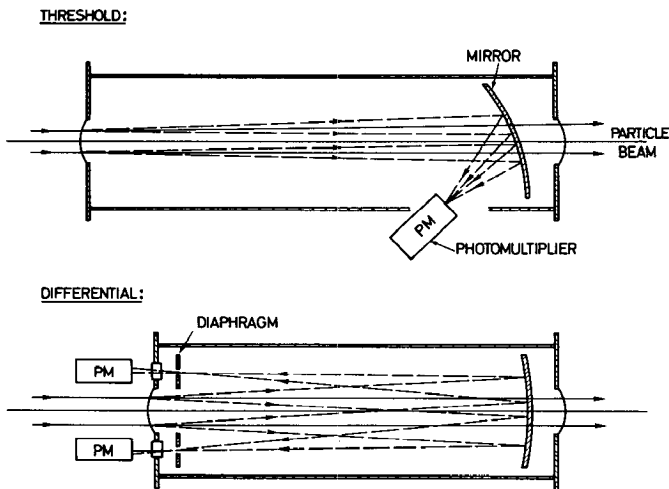


Figure 3 Typical optical systems used in a threshold and a differential Cerenkov counter.

Table 1^a Values of the refractive index, optical dispersion (as defined in equation 14), and multiple scattering factor (equation 19) for some common gas radiators. The wavelengths chosen are those compatible with fused silica optics and S13 or S133 photocathode spectral response.

Gas	Refractive index $(n_0 - 1)10^6$ at 1 atm, 20°C and wavelengths			Optical dispersion ν	Multiple scattering factor $\left[\frac{\rho}{(n_0 - 1)\lambda_0} \right]^{1/2}$ $\text{cm}^{-1/2}$
	$\lambda_1 = 280 \text{ mm}$	$\lambda_2 = 350 \text{ mm}$	$\lambda_3 = 440 \text{ mm}$		
He	33.27	32.90	32.67	54.5	0.24
Ne	64.07	63.37	62.85	52.2	0.67
H ₂	140.6	135.3	132.0	15.7	0.10
N ₂	294.8	287.0	282.0	22.5	0.33
CH ₄	447.8	430.3	419.7	15.3	0.19
CO ₂	447.1	433.3	427.9	19.5	0.32
SF ₆	739.9	727.3	719.4	35.5	0.56

^aThe source of optical data was Landolt-Börnstein, 1962, 6 Auflage, 2 Band, 8 Teil (Springer Verlag). It has been interpolated by the authors.

a mirror onto a single photomultiplier. In the case of the differential counter the reflected ring of Cerenkov light is focused onto an adjustable annular diaphragm. The light passing through the aperture of the diaphragm is detected by a number of photomultipliers equispaced around the annulus. The simplest way to collect the light is by using a lens or a spherical mirror; however a spherical mirror is preferred since it produces less optical aberration.

A spherical mirror of radius of curvature R and focal length $f(=R/2)$ focuses the cone of light in the differential counter into a ring image of radius r , given by

$$r = f \tan \theta \quad 15.$$

The total radial spread Δr of the ring image is then determined by the spherical and coma aberrations which, up to third order, are given by:

$$\Delta r = -\frac{1}{8}(d/f)^3 + \frac{1}{8}(d/f)^2\theta \quad 16.$$

The first term in equation 16 is the spherical error and the second term is due to coma, where d is the useful diameter of the mirror, f is the focal length of the mirror, and θ is the Cerenkov angle. Thus, the angular broadening $\Delta\theta_{\text{OPT}}$ of the ring image due to the optical aberrations is given by

$$\Delta\theta_{\text{OPT}} = \Delta r/f \quad 17.$$

This simple manner of focusing the light is satisfactory in many cases, but to reach the best performance in velocity resolution and angular acceptance the focusing system must be optically corrected. Details of these corrections are given in section 4.

2.7 Energy Loss, Scattering, and Diffraction Effects

As the particle traverses the radiator it loses energy, mainly by the process of ionization, which will alter the value of the velocity β and hence the value of the Cerenkov angle. Multiple Coulomb scattering of the particle causes a broadening of the Cerenkov angle.

The ionization loss, which is about $2 \text{ MeV} \times \text{g}^{-1} \times \text{cm}^{-2}$ for most materials, can in some applications (11) be corrected by varying the refractive index of the radiator along the length of the counter in such a way as to keep the Cerenkov angle constant. This effect soon becomes negligible as the energy increases.

The angular spread $\Delta\theta_{\text{MSC}}$ (root mean squared projected angle) due to multiple scattering of the particle of momentum p can be expressed (12) as

$$\Delta\theta_{\text{MSC}} = (E'/p\beta)t^{\frac{1}{2}} \quad 18.$$

where E' is a constant ($\approx 15 \text{ MeV}$) and t is the length of the radiator in the units of its radiation length. The broadening of the Cerenkov angle has been studied by Dedrick (13) for the case of particles undergoing multiple scattering. Within the approximations of his solution it is concluded that the broadening of the radiation pattern is less than that calculated for the particle trajectory. Thus it is reasonable to use equation 18 as the broadening of the Cerenkov angle.

For a gas radiator of length L , equation 18 can be rewritten as

$$\Delta\theta_{\text{MSC}} = (E'/p\beta)[\rho L(n-1)/\{(n_0-1)X_0\}]^{\frac{1}{2}} \quad 19.$$

where ρ is the gas density, X_0 is the radiation length, and the quantities n , n_0 are defined in equation 10. Values of the quantity $[\rho/\{(n_0-1)X_0\}]^{\frac{1}{2}}$ are included in Table 1 for some commonly used gases. The multiple scattering error, as given by equation 19, is determined by the nature of the radiator and does not depend upon the optical configuration of the counter.

All Cerenkov counters require approximately the same thickness of radiator, expressed in radiation lengths, for a given photoelectron yield irrespective of the design Cerenkov angle. (This is in the approximation that $\gamma\theta > 1$, as shown in Ref. 14.) Since multiple scattering and the magnetic bending of high-energy particles scale like $1/p$, they have the same relative effect on the smearing of the momentum determination of a particle in a given beam-line configuration as the momentum increases.

For the design of Cerenkov counters that require extremely high velocity resolution light diffraction effects eventually give a limit. The broadening of the Cerenkov cone $\Delta\theta_{\text{DIFF}}$ by diffraction is approximately given by:

$$\Delta\theta_{\text{DIFF}} \sim \lambda/(L \sin \theta) \quad 20.$$

For example, for a 5-m differential gas Cerenkov counter operating at $\theta = 25$ mrad and $\lambda = 350$ nm, the broadening $\Delta\theta_{\text{DIFF}} \sim 3 \times 10^{-6}$ rad. If this were the largest contribution to the image spread, the effect on the velocity resolution of the counter would be $\Delta\beta/\beta = \tan \theta \Delta\theta_{\text{DIFF}} \sim 8 \times 10^{-8}$.

2.8 Phase Space Acceptance

In a focusing counter, for example in differential counters and for some threshold counters, the Cerenkov light is directed onto the photocathode via an *imaging* optics and will be detected only if the light passes through the aperture of a diaphragm. For differential counters the aperture is usually an annular slit subtending an angle $\Delta\theta_0$, and for threshold counters can be defined by a single circular aperture placed in front of the photodetector.

The collection of light by the photocathode is therefore simultaneously affected by the value of the angle of emission of the Cerenkov light and the particle divergence with respect to the optical axis of the counter. Thus, all focusing counters accept only particles that are within a limited region of phase space. This reflects the fact that particle identification is achieved through the geometric analysis of the light distribution, uniquely linked to the geometric properties of the particle trajectory.

The acceptance A_c of a focusing Cerenkov counter can be defined as the product of the Liouville invariant (i.e. the beam emittance) and the momentum acceptance such that:

$$A_c = kS_c \Delta\Omega_c \Delta p \quad 21.$$

where S_c is the sensitive area of the photodetector, Δp is the momentum band within which particles collinear with the counter axis can be detected, and k is a factor resulting from the integration. The quantity $\Delta\Omega_c$ is the solid angle subtended by the particles of the central velocity or momentum which are detected such that

$$\theta_0 \Delta \Omega_c = (\pi/4) \Delta \theta_0^2 \quad 22.$$

The acceptance A_b of a beam transport system is a constant of motion for a particle not undergoing acceleration. If there is a Cerenkov counter at some position in this beam the acceptance can be evaluated at any point along the beam, such as at the target position where

$$A_b = S_t \Delta \Omega_t \Delta p = A_c \quad 23.$$

In this relation, the subscript t denotes the values at the target position and k is a numerical factor which has been shown (15) to be equal to $1/3$.

The acceptance of an identified beam that uses a Cerenkov counter is defined by the requirements for mass separation, which thus fixes the value of $\Delta \theta_0$. The largest value of $\Delta \theta_0$ that can be used to detect particles of mass m , when particles of mass $(m + \Delta m)$ are producing light just at the edge of the diaphragm, is given by

$$(\Delta \theta_0/2) \tan \theta = (\Delta \beta/\beta) = (1/\gamma^2) (\Delta m/m) \quad 24.$$

and therefore

$$\Delta \theta_0 \leq (2 \Delta m/m \gamma^2 \tan \theta) \quad 25.$$

A more detailed study of matching a differential Cerenkov counter into a beam design (15) has shown that

$$\Delta \theta_0 \leq (2 \Delta m f/m \gamma^2 \tan \theta) \quad 26.$$

where f is a function limited to values in the range from 0 to 1 depending upon parameters such as target size, collimator size, matrix elements of the beam transport system, beam momentum, mass of the particles under consideration, and the quantity $\tan \theta$ of the differential Cerenkov counter.

The number of secondary particles N_{sec} produced in a target by N_{inc} incident particles is given by

$$N_{\text{sec}} = N_{\text{inc}} (d^2 N/d\Omega dp) \Delta \Omega_b p(\Delta m/m) g \quad 27.$$

where $\Delta \Omega_b$ is the solid angle of the beam and g is an efficiency function with a value between 0 and 1.

The study of the above functions f and g is the basis of the design of a beam system containing particle identification. Such a study has been applied to a charged hyperon beam at CERN, and has shown that a highly efficient identified beam can be obtained. It results that the target size is very important, and because the effective target size is many times larger than its physical size, due to the aberrations of beam optics, the correction of these aberrations is essential.

Two optimum beam configurations are possible. One version can be without a momentum slit, which is therefore a short beam (or a spectrometer), and requires for matching that the angular dispersion of the beam at the counter position be equal to $1/\gamma^2 \tan \theta$. The second version includes a momentum slit, which is a general purpose high-resolution beam, and requires that the angular dispersion at the counter location be zero.

By scaling the length of a differential Cerenkov counter and the value of the Cerenkov angle (14), it is possible to make a beam design that will maintain a good efficiency of particle identification over the energy range from hundreds of MeV up to hundreds of GeV.

3 THRESHOLD CERENKOV COUNTER

The threshold Cerenkov counter detects particles that have a velocity sufficient to produce Cerenkov light in the radiator. The threshold velocity β_0 is defined as that velocity corresponding to a Cerenkov angle $\theta = 0$, that is $\beta_0 = 1/n$ from equation 1. In practice a finite value of the Cerenkov angle is required before the recording efficiency of the photodetector reaches an acceptable value.

To obtain a good detection efficiency it is essential to optimize the circuitry of the photomultiplier and the subsequent discriminator in order to detect single photoelectrons. Due to the statistical fluctuations in the emission of an average number N of photoelectrons from the photocathode, one can define an electronic detection efficiency ε for a counter using a single photomultiplier as:

$$\varepsilon = 1 - \exp(-N)$$

The values of ε are close to unity, i.e. for $N = 4.5$ photoelectrons the quantity $(1 - \varepsilon)$ equals 10^{-2} , and for $N = 6.9$ then $(1 - \varepsilon)$ equals 10^{-3} .

The resolution of a threshold counter is determined by the shape of its efficiency curve near threshold. The slope of this curve is affected by several factors such as the dispersion of the radiator, spread in beam momentum, statistical fluctuation in the number of photoelectrons emitted at the photocathode, and the quality of the counter optics. In general, the resolution can be improved by increasing the photoelectron yield of the counter, that is, by increasing the length of the radiator and maximizing the efficiency for the detection of the Cerenkov photons.

Some Cerenkov detectors with solid or liquid radiators are built to detect the light reaching the boundaries of the radiator at the critical angle. Since values of the critical angles are quite large, the Cerenkov light intensity is also large and hence these counters have a substantial output signal on which to set the threshold. Counters of this type are described in the review articles of Ref. 3.

An important factor in the design of a threshold counter is minimization of the effect of spurious counts due to photomultiplier noise pulses and delta-rays produced in the material of the counter. For counters operating near to the threshold velocity it is often necessary to use at least two counters, and to use the output signals in coincidence. This reduces the effect of photomultiplier noise pulses and, to some extent, the effect of delta-rays, but at the cost of a lower electronic detection efficiency. The number of delta-rays with energies above the threshold can be calculated (12) and, in most cases, is at the level of 10^{-3} of the rate of desired particles.

There have been many ways in which the Cerenkov light has been focused onto the photocathode, such as by using a cylindrical mirror placed around the radiator

(16, 17), light funnels (18), spherical mirrors (19), parabolic mirrors (17), ellipsoidal mirrors (20), or even a Fresnel lens (21).

There have been numerous examples of the threshold detector. In unseparated beams of pions, kaons, and protons, for example, two or three threshold counters can be used to separate the different types of particles. One counter can be set to detect only pions, and a second to detect pions and kaons. Thus it is possible to identify each type of particle in the beam with simple electronics logic. At higher energies, as the thresholds for different particles in a given beam come closer together, it becomes more difficult to use the threshold technique. The effect of spurious signals from noise pulses and from delta-rays make the threshold counter technique unsuitable for some applications.

In recent years the application of threshold Cerenkov detectors has been moving towards higher energies. Only gas radiator threshold counters can be considered in the multi-GeV energy region. For relativistic particles the Cerenkov relation of equation 1 can be rewritten as

$$n(\lambda) - 1 = (1/2)\theta^2(\lambda) + 1 - \beta \quad 28.$$

In equation 8 the velocity difference $\Delta\beta_{m_0m_1}$ between two particles of masses m_0 and m_1 is given in terms of the beam momentum p . Hence if a threshold counter detects the lighter particle of mass m_0 at an average Cerenkov angle $\langle\theta\rangle$, and the heavier particle is at threshold ($\theta = 0$), from equations 8 and 28 it results that:

$$\langle\theta\rangle^2 = 2\Delta\beta_{m_0m_1} = [(m_1^2 - m_0^2)/p^2] \quad 29.$$

assuming that the dispersion in the radiator is small compared to the value of $\langle\theta\rangle$.

From equations 13 and 29 the dispersion in the gas is given by

$$\Delta\theta_{\text{DISP}} = (\langle\theta\rangle/2v)[1 + (1/\gamma_0^2\langle\theta\rangle^2)] \quad 30.$$

and hence,

$$\Delta\theta_{\text{DISP}}/\langle\theta\rangle = (1/2v)[m_1^2/(m_1^2 - m_0^2)] \quad 31.$$

The dispersion does not depend upon p , but is only a function of the masses of the particles. In Table 2 the dispersions have been calculated using equation 31 for some common gases and several particle separations. The values are always small, typically a few percent of the value of $\langle\theta\rangle$, which would not affect significantly the counting rate near threshold.

If one neglects the error due to dispersion for the threshold gas Cerenkov counter, the design parameters can be derived from equations 6 and 29 to be given by

$$\begin{aligned} \langle\theta\rangle &= (N/AL)^{\frac{1}{2}} \lesssim [(m_1^2 - m_0^2)^{\frac{1}{2}}]/p \\ L &\gtrsim (N/A)[p^2/(m_1^2 - m_0^2)] \\ \Delta\beta/\beta_{\text{LIMIT}} &= (\langle\theta\rangle^2/2) = N/2AL \end{aligned} \quad 32.$$

Figure 4 shows a focusing threshold gas Cerenkov counter (22) in operation at the Serpukhov accelerator for secondary-beam particle identification. The Cerenkov

Table 2 Values of the chromatic angular dispersion calculated using equation 31. The values of the optical dispersion parameter ν required for these calculations have been taken from Table 1.

Particle separation		Mass difference ($m_1^2 - m_0^2$) GeV ²	Chromatic dispersion $\Delta\theta_{DISP}/\langle\theta\rangle$		
m_0	m_1		Hydrogen	Nitrogen	Helium
e	μ	0.0112	0.032	0.022	0.009
μ	π	0.0083	0.034	0.024	0.010
π	K	0.224	0.035	0.024	0.010
K	P	0.636	0.044	0.031	0.013
P	Σ^-	0.553	0.083	0.057	0.024
Σ^-	Ξ^-	0.312	0.175	0.111	0.051
Ξ^-	Ω^-	1.051	0.085	0.059	0.024

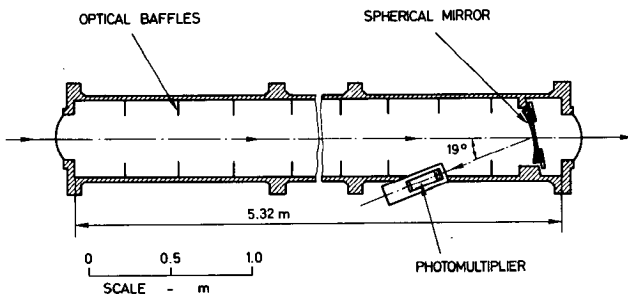


Figure 4 A focusing threshold Cerenkov counter (22) in operation at the Serpukhov accelerator.

light is focused by an inclined spherical mirror of focal length 60 cm onto a single photomultiplier. The spectral range of the detected light is from 180–600 nm. The counter is filled with helium gas and operates at a pressure close to atmospheric for the detection of 50-GeV/c pions. The curves of electronic detection efficiency versus pressure for different values of the photomultiplier high voltage are shown in Figure 5. The velocity resolution, which is defined to correspond to a change in counting efficiency from 0 to 0.63 [i.e. $(1 - \epsilon) = 1/e$], is calculated to be 6.5×10^{-6} . By summing the outputs of two similar threshold counters it was possible to achieve a velocity resolution of 3.6×10^{-6} . The background event rate was less than 3×10^{-4} , and the efficiency on the plateau was better than $(1 - \epsilon) = 6 \times 10^{-7}$.

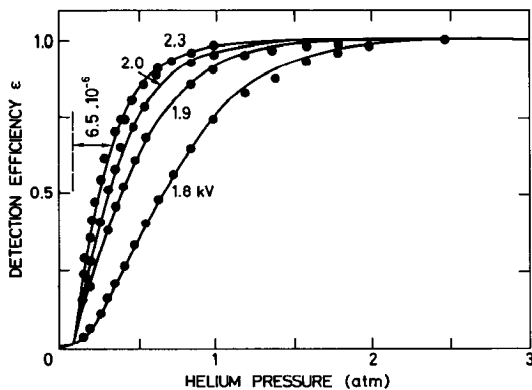


Figure 5 Pressure curves for the threshold counter of Figure 4 in a beam of 50-GeV/c negative pions. The electronic detection efficiency is shown for different values of the photomultiplier high voltage. The velocity resolution is calculated to be 6.5×10^{-6} , corresponding to a change in the efficiency from 0 to 0.63.

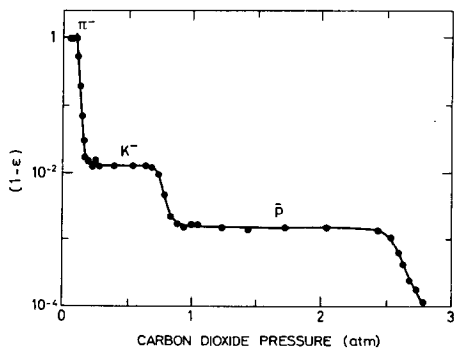


Figure 6 Pressure curve for the threshold counter of Figure 4 in an unseparated 20-GeV/c negative beam. The variation of the parameter $(1-\epsilon)$ is shown as a function of gas pressure. The background level above the antiproton region is about 10^{-6} .

A typical pressure curve for the operation of this counter with a carbon dioxide gas filling and used in a 20-GeV/c unseparated negative beam is shown in Figure 6. The background level above the pressure region for detecting antiprotons is $\sim 10^{-6}$.

There have been several examples of threshold counters detecting particles over a large angular acceptance (23), mostly for the identification of particles emitted from a production target. The light-collection problems are usually simplified by dividing up the acceptance area into several independent counters, consisting of separate

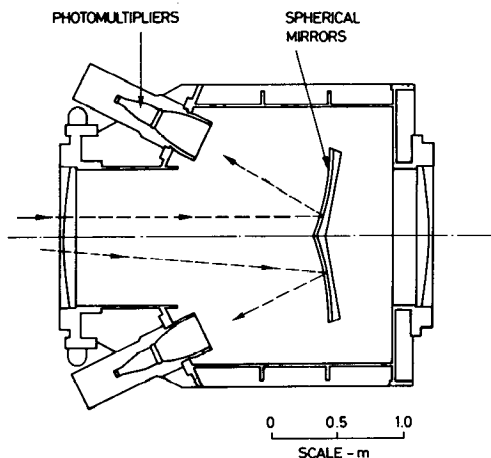


Figure 7 A section through a wide-aperture threshold Cerenkov hodoscope of Williams et al (23). Each of eight spherical mirrors focuses the light onto a separate photomultiplier.

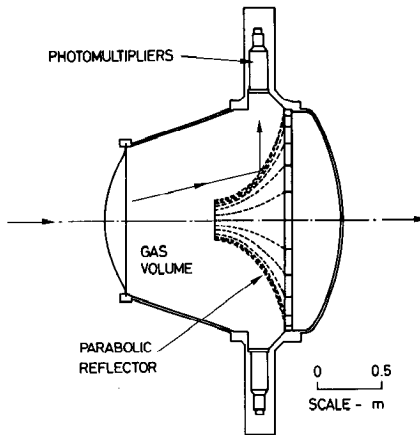


Figure 8 A section through the threshold Cerenkov counter of Ashford et al (23). The particles enter from the left and the Cerenkov light produced by electrons is directed out radially by the reflector onto 24 photomultipliers.

mirrors and photomultipliers. A recent example of this type of counter has been reported by Williams et al (23) and is shown in Figure 7. Each of eight spherical mirrors (62.5 by 62.5 cm) focuses the Cerenkov light onto a separate photomultiplier. Such a counter can be used as eight separate detectors, or the output may be electronically added. This counter has been used to separate $K^+ K^-$ states from $\pi^+ \pi^-$ in an experiment using a 15-GeV pion beam at SLAC.

A large threshold Cerenkov counter has been used by Ashford et al (23) for detecting electrons in experiments of K_{e3} decays and hyperon leptonic decays. A section through the counter is shown in Figure 8. The Cerenkov light emitted in the gas volume is reflected outwards by a sectional parabolic mirror onto a ring of 24 photomultipliers. The detection of pions by this counter was measured to be less than about 0.02%.

4 DIFFERENTIAL CERENKOV COUNTER

The differential Cerenkov counter selects particles of a given velocity by detecting their Cerenkov radiation at a fixed angle. As mentioned in section 2.3, the velocity resolution is given by $\Delta\beta/\beta = \tan\theta\Delta\theta$, where $\Delta\theta$ is the total angular acceptance of the counter. The design of the differential counter can be separated into two main classes depending upon the nature of the radiator; counters using solid or liquid radiators are thus distinguished from counters using a gas radiator.

4.1 Differential Counter Using a Solid or Liquid Radiator

For low-energy particles having $\gamma < 5$, the required refractive index at threshold must be greater than $n = 1.02$, which is inconveniently in the range of compressed

gases. As a consequence of the low value of γ , only a modest velocity resolution of the order of 10^{-2} to 10^{-3} is needed to achieve mass separation of the particles. Thus a solid or liquid material can be considered as the radiator for a differential counter.

The first optical systems for Cerenkov counters were proposed by Getting (24) and discussed in detail in the review by Jelley (3). Several focusing counters have been made using solid or liquid radiators (25). The early counters not only suffered from a poor velocity resolution, but also had a fairly small sensitive area. There followed several designs for counters that could operate in wide particle beams by means of focusing the Cerenkov light (26).

Solid or liquid radiators are available over a range of refractive index, although they cannot be tuned as easily as by varying the pressure of a gas. Therefore, attempts have been made to build an optical system of variable focal length to focus the Cerenkov light emerging from the radiator onto an annular diaphragm. This provides a means of tuning the velocity setting around the value of the refractive index of the radiator.

For some differential counters operating with a small angular spread in an experiment where multiple scattering and energy loss effects are quite small, often the main contribution to the resolution of the counter is the effect of the dispersion in the radiator. This situation can be improved by compensating for the dispersion by means of an achromatic optical system. The general conditions for achromatic optics in Cerenkov detectors were derived by Frank (27) using refraction and reflection at the interface between different media.

An optically corrected and partly achromatic differential Cerenkov counter using a liquid radiator was built by Meunier et al (28) in 1958. Since then about five

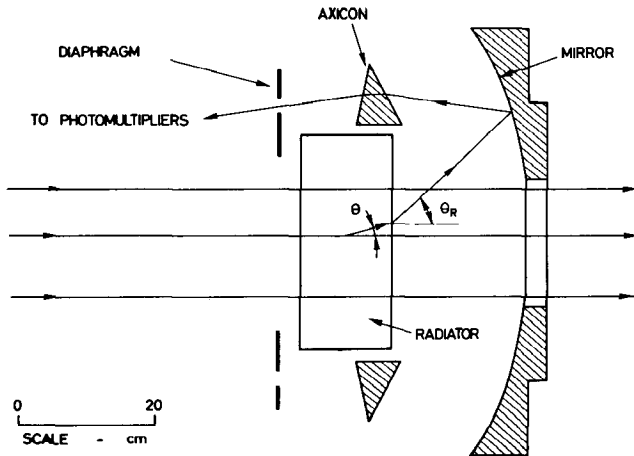


Figure 9 Optics of an achromatic liquid differential counter (DISC) built at CERN (28, 29).

different designs based upon the same principle have been used in experiments at CERN (11, 29). Their design incorporates an exchangeable liquid radiator cell covering a range of refractive index of about 5% (from $n \approx 1.55$ with high-index liquids, to n from 1.33–1.40 with water-glycerine mixtures, to $n \approx 1.28$ using low-index liquids such as FC75). This type of detector has come to be known as a DISC Cerenkov counter (differential isochronous self-collimating).

The principle of the design for the largest liquid DISC counter is shown in Figure 9. The liquid radiator FC75 is contained in a thin cell having a fused silica window. The Cerenkov light is focused by a toroidal mirror of 50-cm radius and passes through a ring-shaped prism onto the aperture of a diaphragm. The light passing through the aperture of the diaphragm is detected by four photomultipliers in coincidence. The ring prism is an axicon lens, that is, it has two conical faces that are described by rotating straight lines around a common optical axis. The axicon not only deflects the Cerenkov light but also compensates for the spread in the cone of light due to dispersion in the radiator.

The light emerging from the exit of the radiator travels at some angle θ_R , which is the refracted Cerenkov angle and not the true Cerenkov angle θ in the radiator. Hence, there exists a relation between θ_R and β given by

$$\tan \theta = \beta \sin \theta_R \quad 33.$$

and hence, from the Cerenkov relation 1, becomes:

$$\sin^2 \theta_R = n^2 - (1/\beta^2) \quad 34.$$

The optical aberrations in this type of counter have to be carefully minimized. The requirements of the optics are that for a single displacement of the axicon lens along the axis: (a) the focal length is altered to cover a range of θ_R , (b) the focal length remains fixed, (c) geometric aberrations are corrected, and (d) chromatic aberrations are corrected. These requirements have been met in the design of the toroidal mirror and axicon lens. The necessary optical precision can be obtained using a mirror and lens made of plastic.

The counter shown in Figure 9 focuses a small angular interval within the range from $40.5^\circ < \theta_R < 50.6^\circ$, and is tuned to a given velocity by moving the position of the axicon relative to the mirror. Thus, the counter can operate over a range of β values:

i.e. using FC75	$0.91 < \beta < 0.97$
water	$0.85 < \beta < 0.94$
pentane	$0.83 < \beta < 0.88$

The range covered indicates that these counters are used at beam momenta generally below about 5 GeV/c. Another design has been made for the detection of low mass particles (i.e. electrons, muons, and pions) where the β values close to unity are encompassed using an angular range from $54.9 < \theta_R < 60.3$.

The velocity resolution for this type of counter, by differentiating equation 34, is given by

$$d\beta = \beta^3 \sin \theta_R \cos \theta_R d\theta_R \quad 35.$$

The range of angular acceptance $d\theta_R$ is chosen by adjusting a variable aperture diaphragm. With an angular setting of $d\theta_R \approx 10$ mrad, the velocity resolution becomes approximately $\Delta\beta \sim 5 \times 10^{-3}$.

For detecting low-energy particles, the energy loss in the radiator produces a significant deterioration in the performance of the DISC counter. This effect was corrected in the multicell DISC counter of Fischer et al (11) in which each of five cells was filled with a liquid of slightly different refractive index n_i so that the refracted angle θ_R was kept constant according to the relation:

$$n_i^2 = \sin^2 \theta_R + (1/\beta_i^2) \quad 36.$$

For these DISC counters a typical optical resolution ($d\theta_R$) has been about 1 mrad for the smallest diaphragm aperture size of 0.2 mm. Hence, if we neglect multiple scattering effects and assume that the axicon produces perfect chromatic correction, this type of counter can produce velocity resolutions approaching $\Delta\beta$ values of $\sim 5 \times 10^{-4}$.

In the design of a differential Cerenkov counter using solid or liquid radiators there are several important parameters to be chosen:

1. The velocity resolution with no chromatic correction is, from equation 34, given by

$$\Delta\beta/\Delta\lambda = -\beta^3 n (\Delta n/\Delta\lambda) \quad 37.$$

This should be as small as possible, and should not depend upon other geometric factors (such as the range of θ) in a well-chosen configuration.

2. The largest divergence angle should be chosen for a given velocity resolution. The Cerenkov angle θ and refracted angle θ_R are related in equation 33, which can be rewritten as

$$\Delta\theta = (\Delta\beta/\beta^2)[n^2 - (1/\beta^2)]^{-\frac{1}{2}} \quad 38.$$

Hence the angular acceptance depends only upon β and n , and not on design parameters of the counter such as θ .

3. The effect of multiple scattering on the velocity resolution from equations 6, 7, and 18 can be expressed as

$$\Delta\beta/\beta = \tan \theta \Delta\theta_{MSC} = (15n/p)(N/AX)^{\frac{1}{2}} \quad 39.$$

which is proportional to the refractive index n .

Hence, from the above three points the optimization of the counter design does not depend directly upon the range of the angle θ_R , but only upon the values of β , n , and Δn . The best choice for a liquid will have the smallest value of n and Δn . Thus the design of the counter begins with the choice of the radiator, and then the required velocity range determines the range of θ_R of the optics.

The fluorocarbons are commonly used in these counters due to their low dispersion and transparency at ultraviolet wavelengths. The main disadvantages of these liquids are the high density (multiple scattering) and immiscibility with other liquids.

In some applications (30) a liquid with a low index of refraction, and hence

low multiple scattering, is used, even though this involves some technical problems in building the counter. In this respect liquid hydrogen ($n = 1.11$) and liquid deuterium ($n = 1.13$) have been used as radiators. The increase in angular acceptance of a liquid hydrogen counter as compared with using FC75 would, from equation 39, be a factor of 1.7.

At the upper momentum limit for the liquid or solid radiator differential Cerenkov counter, at say 5 GeV/c, the velocity resolution $\Delta\beta \approx 5 \times 10^{-3}$ can be typical. If the counter is filled with liquid FC75 an angular acceptance at the highest resolution of about 6 mrad can be used—which is about the size of the divergence of typical secondary beams at these momenta. This type of counter is not suitable for application at higher energies.

4.2 Differential Gas Counter

To separate pions and kaons in a high-energy beam of, say, 100 GeV/c requires a velocity resolution of about 10^{-5} . Such a resolution can be obtained with a differential gas Cerenkov counter. At these high energies the effects of multiple scattering and energy loss become less important, and the main contribution to the velocity resolution is due to the dispersion in the radiator.

The differential gas counter contains a spherical lens that focuses the cone of Cerenkov light onto an adjustable annular diaphragm. The light passing through the aperture is detected by a number of photomultipliers in coincidence. Several differential gas Cerenkov counters have been built (31) with velocity resolutions of about 10^{-4} . Even better resolutions can be achieved by using small values of θ and $\Delta\theta$.

The chromatic spread of the Cerenkov light $\Delta\theta_{\text{DISP}}$ due to dispersion is given by

$$\Delta\theta_{\text{DISP}} = (\theta/2v)[1 + (1/\gamma^2)\theta^2] \quad 40.$$

where v is defined as in equation 14. If we assume that this is the largest error in the image, the effect of the dispersion error on the velocity resolution is given by

$$\Delta\beta/\beta = \tan\theta \Delta\theta_{\text{DISP}} \approx (\theta^2/2v) + (1/2v\gamma^2) \quad 41.$$

Using equation 8, the maximum value of the Cerenkov angle is thus defined by

$$\theta^2/v \lesssim [(1/p^2)(m_1^2 - m_0^2)] - (1/v\gamma^2) \quad 42.$$

In this approximation, the design formulae for the differential gas Cerenkov counter simplify to:

$$\begin{aligned} \theta &\lesssim \frac{1}{p} [v(m_1^2 - m_0^2) - m_i^2]^{\frac{1}{2}} \\ L &\gtrsim \frac{N}{A} \left[\frac{p^2}{v(m_1^2 - m_0^2) - m_i^2} \right] \\ (\Delta\beta/\beta)_{\text{LIMIT}} &= \theta^2/2v \end{aligned} \quad 43.$$

where the subscript i refers to the particle (0 or 1) being detected by the counter.

The ultimate resolution using this type of counter is achieved by using the least

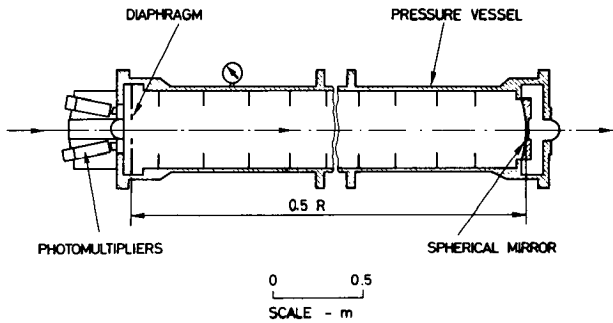


Figure 10 A differential gas Cerenkov counter in use at Serpukhov (32).

dispersive gas, helium. For example, Figure 10 shows a differential gas counter used in the secondary beams at Serpukhov (32). There are two basic designs: one is 5-m long with a Cerenkov angle of 23 mrad, and the second is 10-m long with θ equal to 12 mrad. A velocity resolution of $\Delta\beta < 10^{-5}$ has been achieved by using a helium radiator without correcting for dispersion in the gas. Figure 11

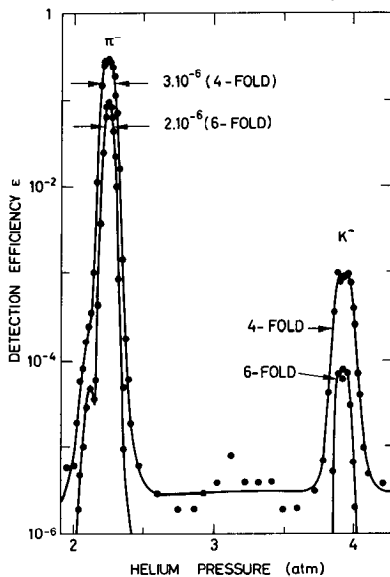


Figure 11 A typical pressure curve for a 10-m gas differential counter, of the type shown in Figure 10, when used in a 45-GeV/c unseparated beam. Results are shown for a 4- and 6-fold coincidence arrangement of the photomultipliers.

shows a typical pressure curve for the 10-m counter when used in a 45-GeV/c beam of pions and kaons. The variation of the detection efficiency is shown when the outputs of the 6 photomultipliers are placed into 6- and 4-fold coincidence arrangements. A background level of better than 1 in 10^6 can be routinely obtained with these counters.

4.3 *Optically Corrected Gas Differential Counter*

It is possible to design optics for the differential gas counter that will correct for the dispersion error by a factor of about 15. This achromatic gas counter (DISC) makes it possible to envisage resolutions in the region of $\Delta\beta \approx 10^{-6}$ to 10^{-7} .

In the differential counter the length of the radiator approximately defines the focal length of the optics. For an acceptable level of detection efficiency and good background rejection (see section 6.1 for further details) at least 24 photoelectrons should be detected by the photomultipliers. Thus, with the length and Cerenkov angle known, it remains to define the required amount of chromatic correction and the range of adjustment of the correction needed for a particular application. Although the correction optics are an added complication, they do provide a counter that can operate over a wide range of operating beam momenta and detect particles over a large mass range. For certain applications, such as in hyperon physics where the constraint on the counter length is severe, it is necessary to use a specially designed achromatic counter.

The required amount of chromatic correction, as given in equation 40, is a function of the velocity of the particle. This variation can be achieved by moving the correction element along the axis of the counter. There is a fairly wide choice of optical configurations that can achieve the correction. The choice is dictated by factors such as complexity of manufacture, number of lens elements, and availability of optical materials.

For a Cerenkov counter the optics must be ultraviolet-transmitting, which excludes all optical glasses except fused silica. There are also some monocrystals which can be used such as NaCl, KCl, CaF_2 , and LiF. However, only NaCl and KCl have a suitable dispersion compared with that of fused silica, and are available in large sizes (up to 350-mm diameter) at a reasonable cost.

Chromatic correction implies that refracting optics will be needed. One can contemplate a design with a single element of fused silica which, in conjunction with a mirror, must have a positive power. However, this combination cannot be tuned to correct over a variable range of chromatism, since the velocity setting of the counter would be affected simultaneously by the corrector lens position and the gas pressure. This solution was possible for the liquid DISC counter (28) because the refractive index in this instance could not be varied. The large Cerenkov angle and the use of an axicon lens in the liquid DISC counter allows the focus to be maintained at a fixed position within an accuracy acceptable for this counter at energies up to about 5 GeV.

The required accuracy for the gas DISC counter is more than two orders of magnitude more precise than for the liquid DISC. The chromatic correction has to be applied in a way that is proportional to $(n-1)$. It is desirable to have a

counter in which the tuning of the velocity setting is independent of the setting of the chromatic corrector. Also, the chromatic corrector should not affect to first order the focal length of the optics for the mean wavelength, irrespective of its longitudinal position, so that the diaphragm can be located at a fixed position. Thus a corrector of zero power is required. One must also incorporate into the design of the corrector the possibility of minimizing longitudinal chromatic aberrations, spherical aberrations, coma, and astigmatism.

The design variables are the curvature, thickness, and positions of all the lenses. The optimization of the design has been performed through a detailed study of ray-tracing for a range of particle velocities, wavelength bandwidths, and corrector positions. In this way an error matrix is developed which must be carefully studied in relation to the effect of these residual errors on the performance of a specific detector.

One type of design that has been shown to be amenable to satisfactory correction over large variations in the design Cerenkov angle from 20 to 120 mrad consists essentially of four elements:

1. A mirror, which is aspheric for counters with small values of Cerenkov angle, and of the Mangin-type for larger angles.

2. A single fused silica lens which, together with the mirror, corrects most of the geometric aberrations. This element also transforms the optics into a telecentric system in which the entrance pupil is at infinity, thus allowing for the stability of the Cerenkov angle even in the presence of some defocusing.

3. A chromatic corrector element (which is a doublet, or preferably a triplet, of fused silica and sodium chloride), which cancels the variation of chromatism by displacement along the counter axis. This element does not affect the velocity setting of the counter.

4. Field lenses of fused silica, used as exit windows, which transfer the light passing through the diaphragm aperture onto the photocathode area of the photomultipliers.

A gas DISC counter was built by Duteil et al (33) with the optics shown in Figure 12. The dispersion was corrected by an achromatic doublet of fused silica and sodium chloride. The Cerenkov angle was 44 mrad and a radiator of 2 m

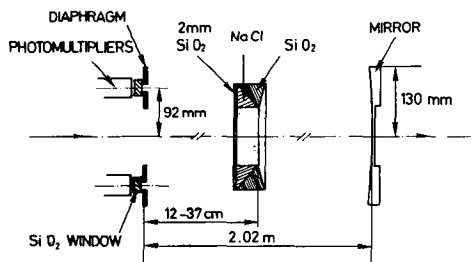


Figure 12 Optics of a gas DISC counter built by Duteil et al (33).

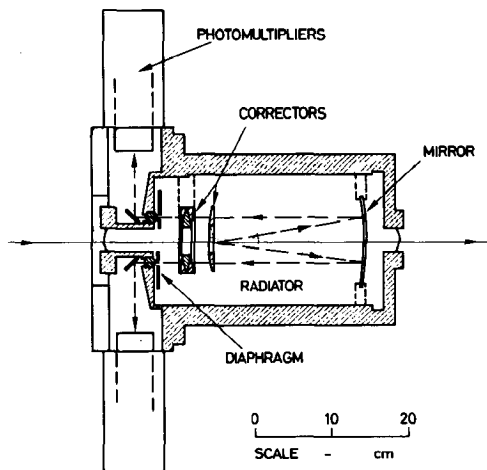


Figure 13 A gas DISC counter used in the 20-GeV charged hyperon beam at CERN (34).

nitrogen (or carbon dioxide) gas was used. A velocity resolution of better than 10^{-5} was achieved with this counter.

An optically corrected gas differential counter operating (34) in the charged hyperon beam at the CERN proton synchrotron is shown in Figure 13. The application of this counter to hyperon physics demanded a high velocity resolution since the Σ^- and Ξ^- particles are close in mass, and the length had to be minimized because the Σ^- half-life is only ~ 57 cm at 20 GeV. Two counters were built with a limiting velocity resolution of 5×10^{-5} covering the range of β from 0.993 to 1.000. The short length was achieved by using a Cerenkov angle of 120 mrad, providing sufficient light in a counter external length of 41 cm.

At this large Cerenkov angle, without optical correction, the geometric aberration would limit the velocity resolution to 2×10^{-4} . The chromatic dispersion alone would limit the velocity resolution to 2×10^{-4} at $\beta = 1.000$, and 4×10^{-4} at $\beta = 0.993$. Since these aberrations are of similar importance, the optics were designed to simultaneously minimize both effects. This was achieved with a design incorporating 6 lenses into a 3-element system, and using spherical surfaces. A Mangin-type mirror was used, consisting of a rear-surfaced aluminized negative meniscus and a single positive meniscus lens. This component removes most of the geometric aberration. A chromatic corrector triplet, which moves along the counter axis to cover the range of β , corrects for the dispersion in the gas radiator. An amount of longitudinal chromatism produced by the chromatic triplet is canceled by introducing a similar amount, but with opposite sign, in the mirror. By a careful evaluation of the correction optics it has been possible to reduce the velocity resolution down to the order of $\Delta\beta \sim 5 \times 10^{-5}$. A typical pressure curve for this DISC counter is shown in Figure 14.

An optically corrected counter is presently under construction for use in the high-energy beams at the NAL and CERN SPS multihundred GeV accelerators. This counter is 5-m long, contains helium gas, and uses a Cerenkov angle of

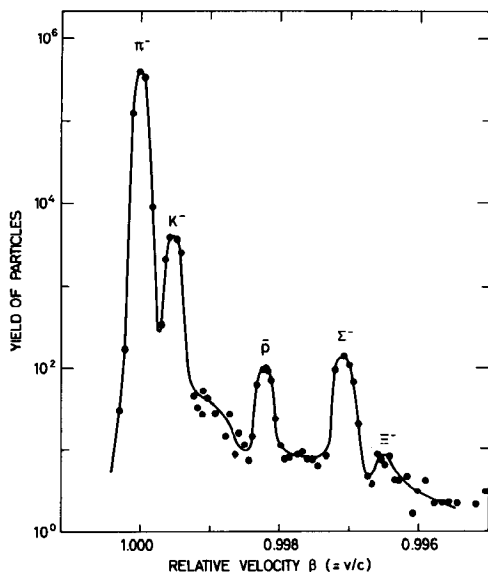


Figure 14 A pressure curve for the DISC counter shown in Figure 13.

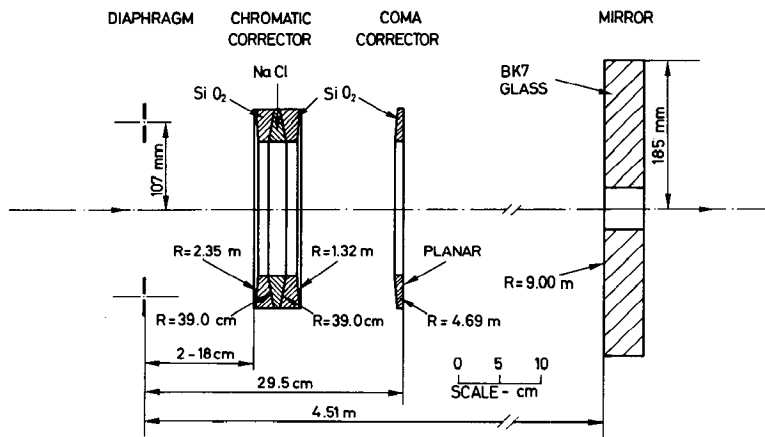


Figure 15 Optics for a gas DISC counter which is to be used in the multihundred GeV beams at NAL and the CERN SPS.

24.5 mrad. The optics are shown in Figure 15. This counter, which is of the type B outlined in Ref. 35, is designed for a velocity resolution of about 4×10^{-7} , which should be capable of distinguishing between pions and kaons in unseparated beams up to about 250 GeV/c. The focusing errors in this counter are about five times larger than the diffraction limit.

It is not so simple to present design equations for the optically corrected differential counters since the correction involves the simultaneous minimization of several kinds of aberrations. However, by studying the several counters already in operation it appears that the limiting velocity resolution is approximately equivalent to having a diaphragm aperture setting that is close to $\Delta r \sim 0.1$ mm ($\pm 50\%$). Hence from this *approximate experimental* fact, the limiting velocity resolution can be expressed as

$$(\Delta\beta/\beta)_{\text{LIMIT}} = \tan \theta \Delta\theta_{\text{LIMIT}} \approx \theta(\Delta r/L) \quad 44.$$

where L is the counter length. Using equations 6, 8, and 44, it is possible to derive an approximate set of design equations for the optically corrected gas differential counter:

$$\begin{aligned} \theta &\approx [N(m_1^2 - m_0^2)/(2A\Delta r p^2)]^{\frac{1}{3}} \\ L &\approx [N/A]^{\frac{1}{3}} [2\Delta r p^2/(m_1^2 - m_0^2)]^{\frac{2}{3}} \\ (\Delta\beta/\beta)_{\text{LIMIT}} &= (A\theta^3 \Delta r/N) \end{aligned} \quad 45.$$

5 COMPARISON OF THRESHOLD AND DIFFERENTIAL CERENKOV COUNTERS

In sections 3 and 4 the design parameters of the threshold and differential Cerenkov counters have been expressed in the form of equations. A comparison of these parameters for counters at high energies, that is for gas counters, is shown in a graphical form (14) in Figures 16–18. The parameters have been calculated using equations 32, 43, and 45. Included in two of these figures are the parameters of four Cerenkov counters presently in operation (32, 34, 36) and three counters currently being designed for use at the CERN SPS (35). The parameters of these selected counters are given in Table 3.

For the curves representing the differential Cerenkov counter, typical values have been used for the ratio (N/A) , as defined in equation 6. The curves for the threshold counter are shown for electronic detection inefficiencies $(1 - \epsilon)$ at the level of 10^{-2} to 10^{-6} . The broken regions in the curves denote that the required gas pressures are in excess of 30 atm for helium or nitrogen, and in excess of 20 atm for the liquefying gas SF_6 . The scale on the abscissa for two of the figures is drawn to show the limiting momentum scale for several pairs of particles. The *limiting momentum* is that value at which the velocity resolution of the counter is equal to the velocity difference between the two particles. In general a Cerenkov counter should not be used at a momentum as high as the limiting value.

Figure 16 shows the maximum values of the Cerenkov angle for the threshold, differential, and DISC types of counter. From equations 32, 43, and 45 the maximum

Table 3 Design parameters for some Cerenkov counters already in operation in high-energy beams or presently in the design stage.

Type	Counter	Ref.	Length m	θ mrad	Gas filling
Differential	IHEP (1)	} 32	5	23	} He, N ₂
	IHEP (2)		10	12	
DISC	CERN (hyperon)	34	0.3	120	SF ₆
	CERN	33	2	44	} CO ₂
	IHEP	36	2.5	45	
	Future designs:	} 35	2	45	SF ₆ , Fr-13
	Type A				
	Type B				
Type C	} 35	5.5	24.5	} He	
		10	20		

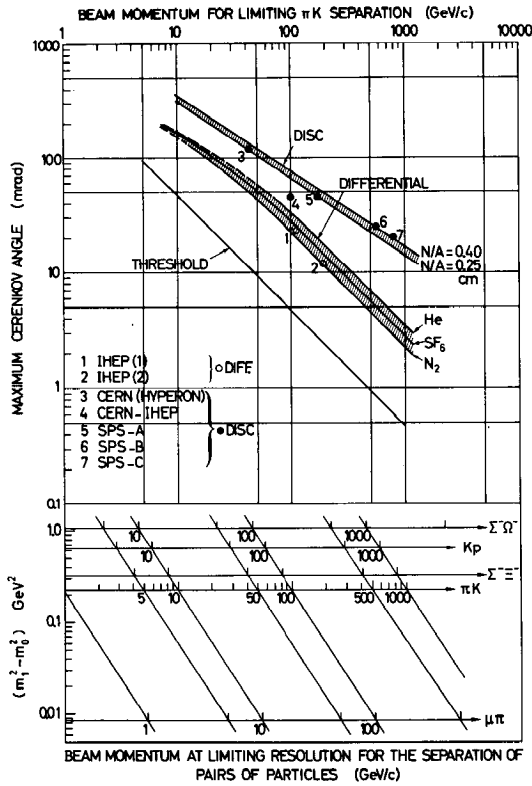


Figure 16 Maximum values of the Cerenkov angle for threshold, differential, and DISC types of gas counters. The abscissa corresponds to values of the beam momenta at which the limiting velocity resolution of each counter is equal to the velocity difference between pairs of particles. The seven Cerenkov counters included in this figure are listed and referenced in Table 3.

values of the angles for these three types of counter scale with the limiting momentum as p^{-1} , p^{-1} , and $p^{-\frac{4}{3}}$, respectively.

The variation of the minimum lengths of the three types of Cerenkov counters is illustrated in Figure 17. The minimum lengths scale with limiting momentum as p^2 , p^2 , and $p^{4/3}$ for the threshold, differential, and DISC counters, respectively. If we assume a constant value of (N/A) , the minimum lengths of the threshold and differential counters are approximately related by

$$L_{\text{THRESH}} \approx vL_{\text{DIFF}} \quad 46.$$

Thus, even if we allow for a smaller value of N for the threshold counter, the

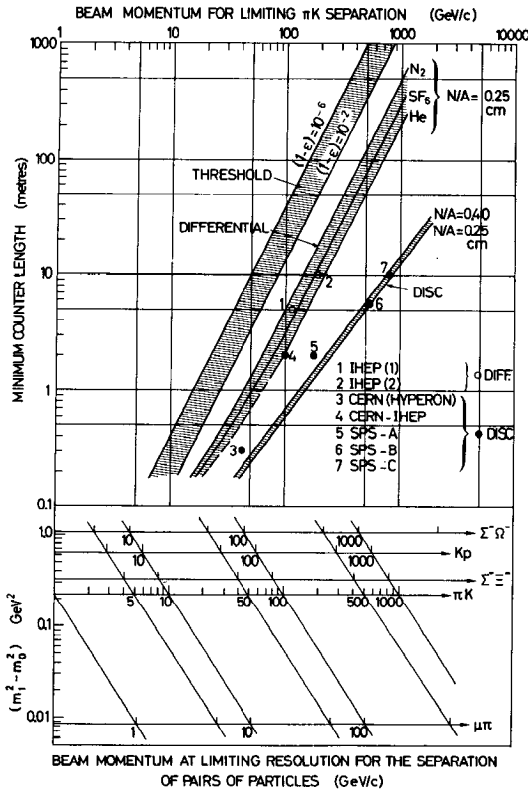


Figure 17 Variation of the minimum lengths of threshold, differential, and DISC Cerenkov counters as a function of the beam momentum for the limiting separation of different pairs of particles.

length of the threshold counter will always be several times the length of a differential counter.

The limiting velocity resolution $(\Delta\beta/\beta)_{LIMIT}$ is shown as a function of the Cerenkov angle θ in Figure 18 for the three types of counters. From the design equations, the limiting resolutions for the threshold, differential, and DISC counters scale as $\langle\theta\rangle^2$, θ^2 , and θ^3 , respectively.

In summary, the gas threshold Cerenkov is the least expensive counter to build as it only requires an average-quality optical mirror, a single photomultiplier, and simple electronic configuration. The counter vessel need only withstand working pressures from vacuum to a few atmospheres, and only a simple refractive index measurement is needed. However, for a given rejection the threshold counter becomes extremely long as the beam energy increases, and therefore these counters have a poorer rejection than the differential counters. There can be counting rate problems,

especially in a veto counter, since all charged particles above threshold (wanted and unwanted) will produce light.

The differential and DISC counters are more precise instruments and, especially the latter, can be designed for the ultimate in velocity resolution at high energies. These counters are relatively more expensive than the threshold counter since they require a higher mechanical precision, especially in the diaphragm, and a high-quality optical mirror. The multicoincidence photomultiplier arrangement demands a substantial amount of fast electronic logic, and the fine velocity resolution requires a precision interferometer for the refractive index measurement. Special optics are needed to correct for the geometric and chromatic aberrations in the DISC counter.

The differential and DISC counters provide a positive signature of particles falling within the accepted velocity band. These detectors are not primarily designed for 100% efficiency, which would be difficult to obtain with multicoincidence logic, but to achieve a very good rejection of particles outside the acceptance in velocity and angle defined for the counter.

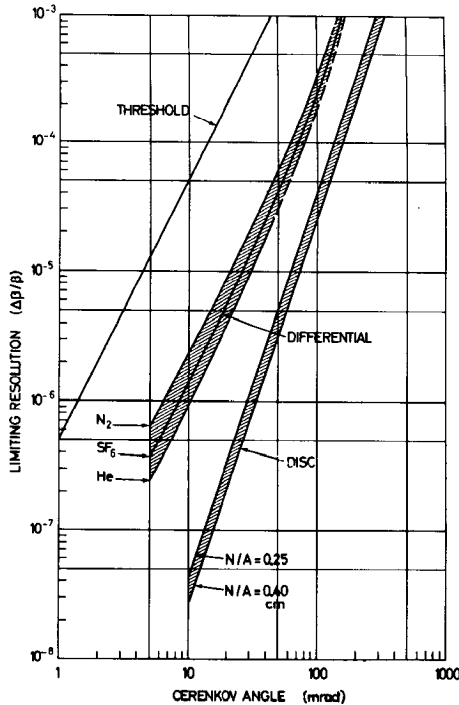


Figure 18 The limiting velocity resolution as a function of the Cerenkov angle for threshold, differential, and DISC types of gas counters.

Annu. Rev. Nucl. Sci. 1973.23:1-44. Downloaded from arjournals.annualreviews.org by HARVARD COLLEGE on 02/28/05. For personal use only.

Threshold counters are generally built to have a good detection efficiency. This is especially important for detecting a particle that is not the lightest mass in the beam. In this case one threshold counter must be used as a veto signal to reject the lighter particles.

At their limiting resolutions the differential and DISC counters have a more restricted angular acceptance than the threshold counter. However, the limiting resolution is needed only in *exceptional cases* where one is prepared to trade acceptance for resolution.

6 PATTERN RECOGNITION IN A FOCUSING CERENKOV COUNTER

6.1 Ring Image Detector

An objective lens using spherical optics will transform Cerenkov light rays emitted at an angle $\theta(\lambda)$ along a particle trajectory into a ring image of radius r in the focal plane of the lens, as shown in Figure 19, such that

$$r = f \tan \theta(\lambda) \quad 47.$$

where f is the focal length of the lens.

The image may suffer from optical aberrations which, if required, can be corrected by using refracting optics such that the quantity $dr/d\lambda$ becomes zero. The Cerenkov photons emitted by the passage of the charged particle will be distributed around the ring image which will then be transformed into a smaller number of photoelectrons by the photodetector. From the geometry of the light dots in the focal plane the velocity and direction of the particle can be obtained. There is therefore a problem of pattern recognition. The radius of the circle and its center must be found for an image defined by random points with a radial distribution which is not necessarily Gaussian.

There have been many attempts to record the dots of light directly onto a photographic plate, and such a method has been used when working with a well-focused beam of monoenergetic particles (37). To detect light from single events it has been necessary to use an image intensifier (38). The best and most recent example is by Giese et al (38) where a velocity resolution of $\Delta\beta = 6 \times 10^{-7}$ has been observed

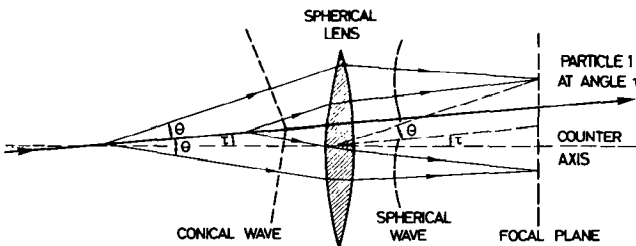


Figure 19 Principle of ring-focusing of Cerenkov light using a spherical lens.

with a systematic error of $\pm 2 \times 10^{-7}$. They used a four-stage cascade image intensifier and recorded the output screen image using photographic film. With a radiator of 10-m helium gas and using $\theta = 11.5$ mrad they obtained a mean value of 1.8 spots of light for each particle. From equation 6 this is equivalent to having an A parameter of 13.6 cm^{-1} , which is quite low when compared with photomultiplier detection but is due to their restricted wavelength bandwidth from 360 to 480 nm at half maximum.

The pattern recognition of a circle requires at least three spots of light, and for this case the fit is always perfect. Giese et al selected events in which at least four spots were evenly spaced around the circumference of the ring, thus reducing the fraction of good events to 5%. The selection of events in this manner leads to the above value of the velocity resolution. This is clearly an off-line procedure and is rather slow.

A simple alternate method is to detect the light that passes through an annular diaphragm placed in front of a photodetector. For detection by a single photodetector the level of discrimination must be higher than a few photoelectrons so as to reduce the number of spurious noise signals, and there is no guarantee that the circle of light does not extend into the opaque part of the diaphragm. This method can produce results for particles that are collinear with the axis, but will never achieve a very low efficiency for particles that are slightly offset in velocity or collinearity (i.e. it will provide a poor rejection of unwanted events).

An improvement is collection of the light falling outside the annular aperture and using this signal in anticoincidence (39). This method suffers from the difficulty that if the anticoincidence threshold is set very low, even the tail of the light distribution that passes through the diaphragm aperture can trigger the anticoincidence channel and thus reduce the efficiency and the effective aperture of the diaphragm. When analyzing less-abundant particles (such as kaons) close to abundant particles (pions), the anticoincidence channel might become overloaded, thus reducing the count rate of the wanted particles. In fact, the anticoincidence method has never achieved a very good quality of rejection of unwanted particles.

A more useful method is to fragment the annular diaphragm into several sectors (q), each connected to a photomultiplier. It can be required that all sectors (or a fraction of the sectors) give an output signal before an event is selected (see Huq & Hutchinson, 26). With all q photomultipliers in coincidence, the accidental background rate due to spurious noise pulses soon becomes negligible as q increases, even when the photodetectors are set to fire on single photoelectrons. Also the q outputs can be grouped in parallel, i.e. the outputs from p adjacent photomultipliers are passed into an *or* circuit, and the outputs from q/p *or* circuits are arranged in coincidence. These different configurations have different efficiencies ε given for example by

$$\begin{aligned} q\text{-fold } \varepsilon &= [1 - \exp(-N/q)]^q \\ q/p\text{-fold } \varepsilon(q, p) &= [1 - \exp(-Np/q)]^{q/p} \end{aligned} \quad 48.$$

where N is the average total number of photoelectrons produced. If an on-line record is made of the counts in these different channels it is possible to continuously

extract the value of ε , and hence N . The background and rejection can also be obtained from the comparison of $\varepsilon(q, p)$ in the region of the mass spectrum between the particle peaks.

The efficiency for the q -fold coincidence requirements (i.e. assuming $p = 1$) is shown in Table 4 as a function of the value N . These efficiencies are generally at the level of 70 to 90%. A higher efficiency can be obtained by using a longer counter, but this is not a recommended choice in view of the fast rising cost and the increased amount of material in the beam.

Table 4 Electronic detection efficiencies for different values of the q -fold coincidence and for values of the average number of photoelectrons N , calculated using equation 48 assuming $p = 1$.

Efficiencies	$N = 12$	$N = 24$	$N = 48$
$q = 3$ fold	0.946	0.999	1.000
4	0.815	0.990	1.000
6	0.418	0.855	0.998
8	0.133	0.665	0.985

The slope of the velocity resolution curve increases as the value of q is increased. For $q > 4$, a q -fold coincidence signal implies that the light ring must be completely included in the diaphragm aperture. It is only this configuration that makes the counter *self-collimating*, that is, insensitive to particles having a divergence greater than $\Delta\theta/2$.

The expected response of a differential or DISC counter versus the number of coincidences q , the total number of photoelectrons N , and the diaphragm angular aperture D (expressed in units of the width of the light spread $\langle\Delta\theta\rangle$) has been computed (15), and a sample of the results is shown in Figure 20. A Poisson distribution is assumed for the distribution of N and for the radial distribution of the intensity of the ring image. Although this assumption is a reasonable approximation of the spread due to multiple scattering and geometric aberrations, it is not strictly valid for the chromatic spread in an uncorrected differential counter, nor is it true for the residual chromatic spectrum in a DISC counter. However, the results of the analysis do provide some conclusions that are in agreement with the experience of running these detectors:

1. The slope of the sides of the peaks is governed by the magnitude of the angular spread $\langle\Delta\theta\rangle$ of the light distribution, and is practically independent of q .
2. The width of the curves depends strongly upon q .
3. The detection efficiency on the peak shows a developing plateau only when the diaphragm angular aperture D is set at more than twice the angular spread $\langle\Delta\theta\rangle$ of the light.
4. It is rather misleading to quote the velocity resolution as the width at half-height of the detection efficiency curves. An ideal Cerenkov counter would present

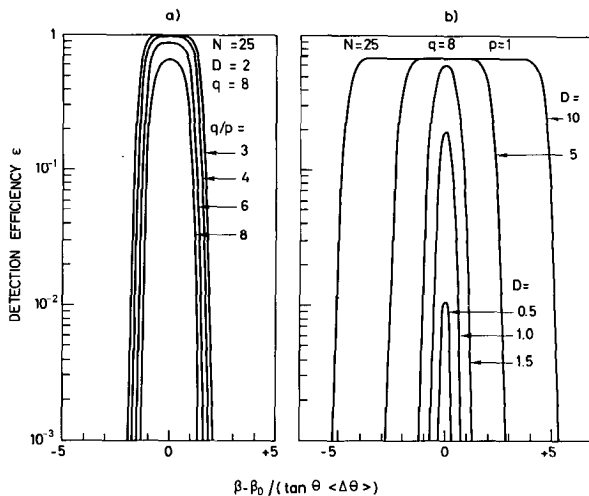


Figure 20 Calculated response curves for a differential or DISC Cerenkov counter as a function of the number of inputs (q/p) to the coincidence circuit and angular aperture of the diaphragm setting (D). The abscissa is a velocity-difference scale expressed in units of the velocity resolution of the counter. N is the number of photoelectrons detected by the total number (q) of photomultipliers.

a rectangular response curve, with a flat top, and would be capable of rejecting particles to the side even with a large width of the curve.

From curves similar to those shown in Figure 20 it is apparent that a good compromise for the working conditions is setting the diaphragm at two or three times the value of $\langle \Delta\theta \rangle$, and choosing the total number of the groupings (q/p) of the photomultipliers to be greater than about 6. This compromise ensures that there is a small plateau region on the top of the efficiency curve, with an efficiency as given by equation 48, and that there is no sizable degradation of the mass resolving power of the counter. If the value of q is 6 or 8, from Table 4 one can conclude that a value of N of about 24 is recommended to obtain an acceptable counting efficiency.

Actual experimental results can be illustrated by the pressure curve of the IHEP 5-m differential counter (32). Figure 21 shows the counting efficiency curves for two settings of the diaphragm aperture as a function of the number (q/p) of inputs into the coincidence arrangement.

6.2 Spot Image Detector

Another possibility for electronic pattern recognition is focusing the Cerenkov light from a single particle to form a single dot of light, a technique which has been applied since the start of the development of Cerenkov counters (24, 40). The focusing conditions for a dot are such that for a narrow particle beam they are

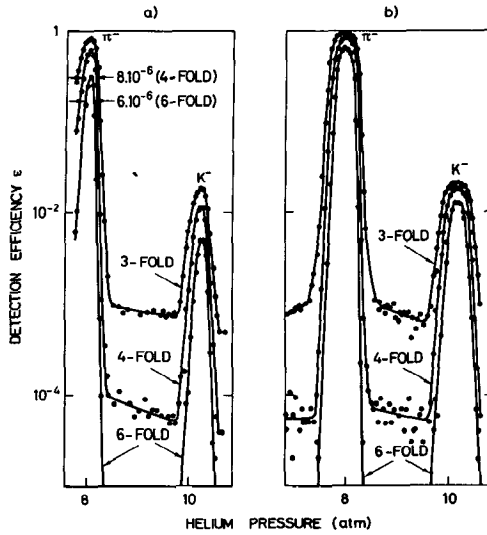


Figure 21 Pressure curves for the IHEP 5-m differential Cerenkov counter (32) illustrating quality of detection, and rejection of unwanted events, in an unseparated 40-GeV/c negative beam. The detection efficiency is shown as a function of the number of inputs into the coincidence arrangement for the two diaphragm slit settings of (a) 1.6 mm and (b) 3.2 mm.

approximately obtained through the use of conical, cylindrical, or more complicated revolution surfaces, all having a singular point on the axis. This focusing, although approximate, was sufficient for the precision required from liquid or solid radiators with particles of about 100 MeV. For particles outside the velocity acceptance band the spot enlarges and falls outside the region defined by a circular diaphragm.

The spot-focusing idea has been recently revived in a computer study of a proposed

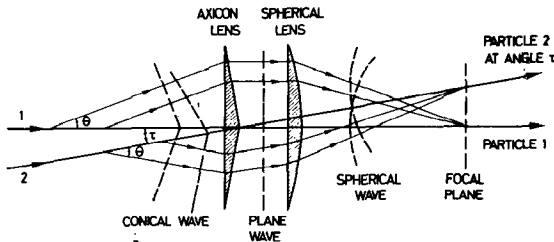


Figure 22 The principle of the spot-focusing of Cerenkov light using an axiconic lens to produce a plane wavefront, followed by a spherical lens to form the final point image in the focal plane.

counter design by Benot et al (41). The principle of the counter optics is illustrated in Figure 22. The conical wavefront of the Cerenkov light is converted into a plane wavefront using an axicon lens, and the final image is formed by a spherical lens. The counter can detect *multiparticle* production as long as the position of the target coincides with the position of the apex of the axicon (or a virtual image of the axicon). The Cerenkov light from a particle of velocity β_0 is focused to a spot, whereas light from a particle of velocity different from β_0 produces a ring image. Benot et al have studied a possible design for this type of detector which, assuming a production target of 1-mm radius, is capable of providing the angular coordinates of multiparticles to ± 0.1 mrad and the velocities (in the range of $70 < \gamma < 400$) to $\Delta\beta \approx 2 \times 10^{-6}$.

The spot-focusing idea offers the possibility of simultaneously detecting the particle velocity and direction. This is a clear advantage over the crude pattern recognition afforded by the single annular diaphragm of a differential Cerenkov counter.

6.3 Multiplexed Cerenkov Counter

The restricted phase-space acceptance of a differential counter with a single diaphragm is a drawback in the measurement of particles coming from an extended phase space (large target size). One way to obtain more data on each event is to multiplex the output of the Cerenkov counter.

A six-channel Cerenkov counter (42) using a specially zoned mirror has been used in a precision measurement of the pion-proton total cross section (43). As shown in Figure 23, the Cerenkov light is focused by a spherical mirror into a ring image at the focal plane. A special spherical mirror is placed in the focal plane to focus the light from each of the six zones onto pairs of photomultipliers connected in coincidence. A particle traveling along the optical axis of the counter, and producing Cerenkov light at an angle θ , will form a ring image at the focal plane of radius $r = f \tan \theta$, and centered on the point O. If a particle enters the counter at an angle α with respect to the optical axis, the center of the ring image is displaced to the

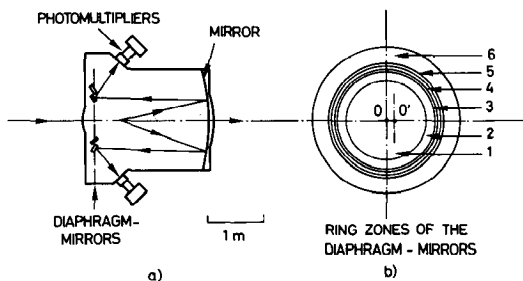


Figure 23 A six-channel Cerenkov counter built by Ivanov et al (42) in which Cerenkov light is focused onto special diaphragm-mirrors in the focal plane of the counter optics. Using a suitable electronic logic between the light outputs from each ring zone of the diaphragm-mirrors it is possible to determine the angle of each incoming particle.

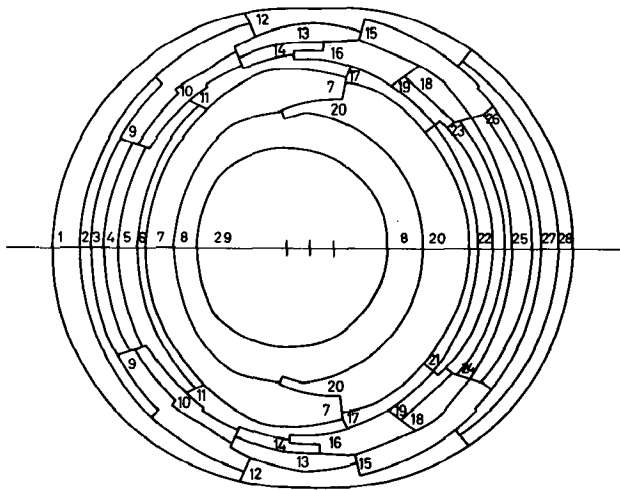


Figure 24 A special mirror proposed for the mass sensitive image-dissecting Cerenkov counter of Roberts (45) planned for use in the charged hyperon beam at NAL.

point O' by an amount equal to $f \tan \alpha$. Hence by using an electronic logic (in coincidence and veto arrangement) of the light outputs detected from each of the six zones it was possible to define the scattering angles α in the experiment.

A more elaborate multiplexed Cerenkov counter with segmented mirror has been proposed by Soroko (44) at Dubna. Also Roberts (45) has designed a mass sensitive image-dissecting Cerenkov counter for the 150-GeV/c charged hyperon beam at NAL. As proposed, the mirror is divided into several segments which are adjusted to focus the Cerenkov light onto 29 photomultipliers. The complexity of the mirror is shown in Figure 24. By a suitable electronic logic, this counter is designed to produce specific trigger signals for a range of particle masses (up to the deuteron mass). A multichannel Cerenkov device is being constructed at Serpukhov (46) in which a diaphragm having variable radius and aperture size is placed in front of each of 12 photomultipliers.

The possibility introduced by special photomultipliers with crossed magnetic and electric fields (47) has been incorporated into the design of a multichannel counter by Vishnevsky et al (48). These photomultipliers provide a determination of the point of emission of the photoelectrons from the output signal delay, and can therefore replace an aperture-diaphragm arrangement.

7 CONCLUSIONS

With the advent of the new accelerator at NAL, physics instrumentation has entered into the multihundred GeV energy range. The possibilities for different

types of particle detectors and identifiers are quite restricted in this new energy range, and will consist mainly of the following devices:

1. Scintillation counters, which provide fast timing (down to ~ 0.1 nsec) and track position information to the accuracy of a few millimeters.

2. Wire chambers, which have a poorer timing accuracy than scintillators but provide accurate position information [down to ~ 0.1 mm for high pressure wire chambers (49) or drift chambers (50)].

3. Total absorption counters or nuclear detectors based upon the emission of scintillation or Cerenkov light in large-size radiators. Unfortunately these detectors make a destructive measurement on the particles but can produce an energy determination approaching the accuracy of a few percent (51).

4. Ionization detectors based upon the measurement of the relativistic rise of the energy loss by ionization. This technique is in an early stage of development (52).

5. Transition radiation detectors, which are also in the developmental stage (53), are particularly suited for the detection of high γ particles. Thus they will be useful in detecting low-mass particles.

6. Cerenkov counters, which can provide velocity and angular coordinates of charged particles over a wide range of masses and beam energies. The effect is well known, and counters can be designed with confidence. Due to the large statistical fluctuation associated with a low light yield, an *intensity measurement* of Cerenkov radiation provides a rather poor result for single particles and is valid only for a large group of particles. However, the usefulness of the Cerenkov detector is that an *angular measurement* of the light, which is not subject to the effect of statistical fluctuations, can produce a high accuracy even for single particles.

The limit for the application of the Cerenkov technique at high energies will be established by the ability to resolve the velocity of the particle with an accuracy that is going approximately as $1/p^2$. In the differential Cerenkov counter the optical aberrations will set this limit, whereas the DISC counter will be limited eventually by the diffraction of light. It appears that practical limits for the application of Cerenkov counters may be reached within the energy range afforded by the new multihundred GeV accelerators at NAL and CERN.

Literature Cited

1. Cerenkov, P. A. 1934. *Dokl. Akad. Nauk SSSR* 2:451
Vavilov, S. I. 1934. *Dokl. Akad. Nauk SSSR* 2:457; *Ibid* 1956. *Sobranie Sochinenii (collected works)* 4:356. Moscow: Izdatel'stvo Akad. Nauk SSSR
2. Tamm, I. E., Frank, I. M. 1937. *Dokl. Akad. Nauk SSSR* 14:107
3. Jelley, J. V. 1958. *Cerenkov Radiation And Its Applications*. London: Pergamon
Hutchinson, G. W. 1960. *Progr. Nucl. Phys.* 8:197-236
4. Zrelov, V. P. 1968. *Cerenkov Radiation In High-Energy Physics*. Moscow: Atomizdat. 2 vols. (English transl.: 1970. *Israel Program Sci. Transl.*)
5. Denisov, S. P. 1971. *Advances in Cerenkov counters*. *IHEP Rep.* 71/47
6. Cerenkov, P. A. 1944. *Tr. Fiz. Inst. Akad. Nauk SSSR* 2:4
Ginsburg, V. L. 1940. *Zh. Eksp. Teor. Fiz.* 10(6):589
Pinsky, L. S., Eandi, R. D., Osborne, W. Z., Rushing, R. B. 1971. *XII Int. Conf. Cosmic Rays, Tasmania* 4:1630-34

7. Lakes, R. S., Poultney, S. K. 1971. *Appl. Opt.* 10: 797-800
8. Duteil, P., Garron, J. P., Meunier, R., Stroot, J. P., Spighel, M. 1968. *CERN Rep.* 68/14
- Yovanovitch, D. D. et al 1971. *Nucl. Instrum. Methods* 94: 477-80
9. Vovenko, A. S. et al 1964. *Sov. Phys. Usp.* 6(6): 794-824
10. Linney, A., Peters, B. 1972. *Nucl. Instrum. Methods* 100: 545-47
11. Fischer, J., Leontic, B., Lundby, A., Meunier, R., Stroot, J. P. 1959. *Phys. Rev. Lett.* 3: 349-50
12. Rossi, B., Greisen, K. 1941. *Rev. Mod. Phys.* 13: 240
13. Dedrick, K. G. 1952. *Phys. Rev.* 87: 891-96
14. Benot, M., Litt, J., Meunier, R. 1972. *Nucl. Instrum. Methods* 105: 431-44
15. Meunier, R. Characteristics of charged particle beams for mass identification using a differential Cerenkov counter. In preparation
16. Bayatyan, G. L., Zel'dovich, O. Ya., Landsberg, L. G. 1964. *Instrum. Exp. Tech.* 7: 805-10
17. Vivargent, M., Von Dardel, G., Mermod, R., Weber, G., Winter, K. 1963. *Nucl. Instrum. Methods* 22: 165-68
18. Hinterberger, H., Winston, R. 1966. *Rev. Sci. Instrum.* 37: 1094-95; *Ibid* 1968. 39: 1217-18
19. Denisov, S. P. et al 1970. *Nucl. Instrum. Methods* 85: 101-7
20. Dobbs, J. MacG., McFarlane, W. K., Yount, D. 1967. *Nucl. Instrum. Methods* 50: 237-41
21. Swanson, R. J., Masek, G. E. 1961. *Rev. Sci. Instrum.* 32: 212
22. Denisov, S. P. et al 1970. *Nucl. Instrum. Methods* 85: 101-7
23. Hinterberger, H. et al 1970. *Rev. Sci. Instrum.* 41: 413-18
- Aubert, J. J. et al 1970. *Rev. Sci. Instrum.* 87: 79-85
- Williams, H. H., Kilert, A., Leith, D. W. G. S. 1972. *Nucl. Instrum. Methods* 105: 483-91
- Ashford, V. et al 1972. *Nucl. Instrum. Methods* 98: 215-20
- Cence, R. J. et al 1973. *Nucl. Instrum. Methods* 108: 113-18
24. Getting, I. A. 1947. *Phys. Rev.* 71: 123-24
25. Chamberlain, O., Segrè, E., Wiegand, C., Ypsilantis, T. 1955. *Phys. Rev.* 100: 947-50
- Huq, M. 1958. *Nucl. Instrum. Methods* 2: 342-47
26. Leontic, B. 1957. *CERN Rep.* 59/14
- Von Dardel, G. 1960. *Proc. Int. Conf. Instrum. High Energ. Phys., Berkeley.* 166-71
- Huq, M., Hutchinson, G. W. 1959. *Nucl. Instrum. Methods* 4: 30-35
27. Frank, I. M. 1956. *Usp. Fiz. Nauk* 58(1): 111
28. Meunier, R., Stroot, J. P., Leontic, B., Lundby, A., Duteil, P. 1962. *Nucl. Instrum. Methods* 17: 1-19, 20-30
29. Dowell, J. D. et al 1962. *Phys. Lett.* 1: 53-56
- Gilly, L. et al 1964. *Phys. Lett.* 11: 244-48
- Gilly, L. et al 1965. *Phys. Lett.* 19: 335-38
- Davies, J. D. et al 1967. *Phys. Rev. Lett.* 18: 62-64
- Davies, J. D. et al 1968. *Nuovo Cimento A* 54: 608-19
- Binon, F. et al *Nucl. Phys. B* 33: 42-60
30. Ayres, D. S. et al 1969. *Nucl. Instrum. Methods* 70: 13-19
31. Mermod, R., Winter, K., Weber, G., Von Dardel, G. 1960. *Proc. Int. Conf. Instrum. High Energ. Phys., Berkeley.* 172-73
- Kycia, T. F., Jenkins, E. W. 1961. *Proc. Conf. Nucl. Electr., Belgrade* 1: 63-70
32. Denisov, S. P. et al 1971. *Nucl. Instrum. Methods* 92: 77-80
33. Duteil, P., Gilly, L., Meunier, R., Stroot, J. P., Spighel, M. 1964. *Rev. Sci. Instrum.* 35: 1523-24
34. Badier, J. et al 1972. *Phys. Lett. B* 39: 414-18
35. Meunier, R. 1970. *NAL Summer Study Rep. SS/170*, 85-108
36. Bushnin, Yu. B. et al 1971. *Instrum. Exp. Tech.* 14: 67
37. Zrelov, V. P. 1963. *Instrum. Exp. Tech.*, 6: 215-19
- Zrelov, V. P., Pavlovic, P., Sulek, P. 1972. *Nucl. Instrum. Methods* 105: 109-16
38. Roberts, A. 1960. *Nucl. Instrum. Methods* 9: 55
- Butslov, M. M., Medvedev, M. N., Chuvilo, I. V., Sheshunov, V. M. 1963. *Nucl. Instrum. Methods* 20: 263-66
- Reynolds, G. T., Waters, J. R., Poultney, S. K. 1963. *Nucl. Instrum. Methods* 20: 267-70
- Binnie, D. M., Jane, M. R., Newth, J. A., Potter, D. C., Walters, J. 1963. *Nucl. Instrum. Methods* 21: 81-84
- Benwell, R. 1964. *Nucl. Instrum. Methods* 28: 269-73
- Iredale, P., Hinder, G. W., Parham, A. G.,

- Ryden, D. J. 1966. *Advan. Electron. Electron Phys. B* 22: 801-12
- Giese, R., Gildemeister, O., Paul, W., Schuster, G. 1970. *Nucl. Instrum. Methods* 88: 83-92
39. Kycia, T. F., Jenkins, E. W. See Ref. 31
- Lindenbaum, S. J., Love, M., Ozaki, S., Russell, J., Yuan, L. C. L. 1963. *Nucl. Instrum. Methods* 20: 256-60
40. Marshall, J. 1952. *Phys. Rev.* 86: 685-93; *Ibid* 1954. *Ann. Rev. Nucl. Sci.* 4: 141-56
- Ozaki, S., Russell, J. J., Sacharidis, E. J. 1965. *Nucl. Instrum. Methods* 35: 301-8
41. Benot, M., Howie, J. M., Litt, J., Meunier, R. 1973. A spot-focusing Cerenkov counter for the detection of multiparticle events at high energies. Unpublished
42. Ivanov, V. I., Moroz, N. S., Radomanov, V. B., Stavinsky, V. S., Zubarev, V. N. 1970. *JINR Rep. E13/5459, Dubna*
43. Giordenesku, N. et al 1970. *JINR Rep. P1/5460, Dubna*
44. Soroko, L. M. 1971. *JINR Rep. P13/6019, Dubna*
45. Roberts, A. 1972. *Nucl. Instrum. Methods* 99: 589-98
46. Vorontsov, V. L., Goldberg, G. R., Denisov, S. P., Kudrjashov, A. M., Lifshits, E. M. 1968. *Bull. Izobretatelja, N36*
47. Aleksandrova, N. F. et al 1969. *IHEP Rep. 69/22, Serpukhov*
48. Vishnevsky, N. K. et al 1970. *Proc. Int. Conf. Instrum. High Energ. Phys., Dubna* 1: 305-20
49. Willis, W. J., Hungerbuchler, V., Tanenbaum, W., Winters, I. J. 1971. *Nucl. Instrum. Methods* 91: 33-36
50. Charpak, G., Rahm, D., Steiner, H. 1970. *Nucl. Instrum. Methods* 80: 13-34
- Charpak, G. 1970. *Proc. Int. Conf. Instrum. High Energ. Phys., Dubna* 1: 217-50
- Charpak, G., Sauli, F., Duinker, W. 1973. High accuracy drift chambers and their use in strong magnetic fields. Unpublished
51. Hughes, E. B., Hofstadter, R., Lakin, W. L., Sick, I. 1969. *Nucl. Instrum. Methods* 75: 130-36
- Hayashi, M., Homma, S., Kajiura, N., Kondo, T., Yamada, S. 1971. *Nucl. Instrum. Methods* 94: 297-99
- Engler, J. et al 1973. *Nucl. Instrum. Methods* 106: 189-200
52. Landau, L. D. 1944. *J. Phys.* 6: 201-5
- Vavilov, P. V. 1957. *Sov. Phys. JETP* 5: 749-51
- Blunck, O., Westphal, K. 1951. *Z. Phys.* 130: 641-49
- Dimčovski, Z., Favier, J., Charpak, G., Amato, G. 1971. *Nucl. Instrum. Methods* 94: 151-55
53. Garibian, G. M. 1960. *Sov. Phys. JETP* 37(10): 372-76
- Garibian, G. M. 1970. *Proc. Int. Conf. Instrum. High Energ. Phys., Dubna* 2: 509-29
- Alikhanian, A. I., Avakina, K. M., Garibian, G. M., Lorikian, M. P., Shikhliarov, K. K. 1970. *Phys. Rev. Lett.* 25: 635-39
- Wang, C. L., Dell, G. F. Jr., Uto, H., Yuan, L. C. L. 1972. *Phys. Rev. Lett.* 29: 814-17
- Bamberger, A., Dell, G. F. Jr., Uto, H., Yuan, L. C. L., Alley, P. W. 1973. *Phys. Lett. B* 43: 153-56
- Alikhanian, A. I., Kankanian, S. A., Oganessian, A. G., Tarnanian, A. G. 1973. *Phys. Rev. Lett.* 30: 109-11
- Harris, F. et al 1973. *Nucl. Instrum. Methods* 107: 413-22

CONTENTS

CERENKOV COUNTER TECHNIQUE IN HIGH-ENERGY PHYSICS, <i>J. Litt and R. Meunier</i>	1
PHOTON-EXCITED ENERGY-DISPERSIVE X-RAY FLUORESCENCE ANALYSIS FOR TRACE ELEMENTS, <i>F. S. Goulding and J. M. Jaklevic</i>	45
FLASH-TUBE HODOSCOPE CHAMBERS, <i>Marcello Conversi and Gennaro Brocco</i>	75
SYMMETRIES IN NUCLEI, <i>K. T. Hecht</i>	123
LINEAR RELATIONS AMONG NUCLEAR ENERGY LEVELS, <i>Daniel S. Koltun</i>	163
INTERMEDIATE STRUCTURE IN NUCLEAR REACTIONS, <i>Claude Mahaux</i>	193
PRODUCTION MECHANISMS OF TWO-TO-TWO SCATTERING PROCESSES AT INTERMEDIATE ENERGIES, <i>Geoffrey C. Fox and C. Quigg</i>	219
THE RADIATION ENVIRONMENT OF HIGH-ENERGY ACCELERATORS, <i>A. Rindi and R. H. Thomas</i>	315
RADIOACTIVE HALOS, <i>Robert V. Gentry</i>	347
THE MANY FACETS OF NUCLEAR STRUCTURE, <i>Aage Bohr and Ben R. Mottelson</i>	363
MOLECULAR STRUCTURE EFFECTS ON ATOMIC AND NUCLEAR CAPTURE OF MESONS, <i>L. I. Ponomarev</i>	395
SOME RELATED ARTICLES APPEARING IN OTHER ANNUAL REVIEWS	431
REPRINT INFORMATION	433
AUTHOR INDEX	435
CUMULATIVE INDEX OF CONTRIBUTING AUTHORS, VOLUMES 14 TO 23	443
CUMULATIVE INDEX OF CHAPTER TITLES, VOLUMES 14 TO 23	444